NASA CR-172,489

NASA Contractor Report 172489

NASA-CR-172489
19850012863

Automatic Control Design Procedures for Restructurable Aircraft Control

D.P. Looze, S. Krolewski, J.L. Weiss,
N.M. Barrett, and J.S. Eterno

Contract NAS1-17411

January 1985

NASA
National Aeronautics and Space Administration

Langley Research Center
Hampton, Virginia 23665

ALPHATECH, INC.
2 BURLINGTON EXECUTIVE CENTER
111 MIDDLESEX TURNPIKE
BURLINGTON, MA 01803
617-273-3388

CONTENTS

CONTENTS (Continued)

FIGURES

FIGURES (Continued)

SECTION 1

INTRODUCTION AND RESEARCH PERSPECTIVE

1.1 OVERVIEW

The research under this contract has been directed at the problem of automatically reconfiguring the remaining control effectors of an aircraft that has suffered one or more control effector failures. This problem has been motivated by several recent incidents involving commercial aircraft [1], [2]* and has drawn a considerable amount of preliminary attention [3],[14].

As aircraft become increasingly sophisticated, and as static stability is decreased in the interests of efficiency and maneuverability, the potential damage caused by unanticipated failure increases dramatically. Although pilots can be trained to react in the case of anticipated major failures, they cannot be expected to respond correctly, and in time, for all conceivable failures. This is particularly frustrating because modern aircraft, with complex controls, may remain controllable despite individual failures, as happened recently in two well publicized cases. In one case, (a Delta L1011 flight [2]) the pilot was able to reconfigure his available controls to save the plane. In another, (the Chicago DC10 crash [1]) the pilot could not, although hindsight revealed the plane could have been saved.

The objective of the restructurable controls research is to automatically and quickly solve the control problem facing a pilot during an emergency.

*References are indicated by numbers in square brackets; the list appears at the end of of this report.

The class of problems of interest includes those where the failure or failures are unanticipated, but excludes those unsolvable areas (wings falling off) where the plane cannot be saved.

The general area of emergency control modification can be divided into two categories: reconfigurable and restructurable control. The first category includes failures which can be anticipated and solved in advance such as engine or instrument failures. The most important failures in this class are analyzed and pilots are trained in emergency procedures to compensate for them. The major advances in reconfigurable controls in the near future may be expected to occur in computer storage and automatic activation of pre-solved emergency procedures. This involves computerizing "the book", and ensuring that emergency procedures do not simply rely on pilot training and memory under stress.

The second class of problems, and the one of interest here, includes those emergencies which cannot easily be anticipated and planned for. It includes those cases where "the book" must be thrown out. Ideally, the solution to this class of problems would place the experience and expertise of the best pilots and aircraft designers immediately at the disposal of the pilot in trouble. Such experts (or their artificial intelligence embodiments) would analyze the problem and recommend solutions (some, perhaps, unconventional). Their actions would return the aircraft to a safe operating condition, and they would remain available to answer "what if" questions for the remainder of the flight, in particular involving changes to the aircraft to prepare for landing.

This assembly of experts would, in fact, be answering the following questions:

1. Did a failure occur?

2. What failure(s) occurred?

3. How can I restructure the controls to accommodate the failure(s)?

4. What else will happen if I change the controls?

The first two questions constitute failure detection and identification, (FDI) and have received much research interest in the last decade [4]. Automatic techniques exist for determining whether a failure has occurred and for isolating the failure component. In addition, current research is underway for designing robust FDI systems which can accomplish their mission with "real world" plant uncertainty and disturbances.

If a new aircraft model were available from an FDI system, a reliable automatic procedure would be required to answer the third and fourth question. In essence, the answer to these questions is a redesign of the flight control system (FCS) of the aircraft. The objective of the research presented in this report is to begin the development of an automatic FCS redesign procedure that is both reliable and fast.

The key features of the restructurable control problem that an automatic redesign procedure must address are:

1. the failures are unanticipated;

2. the available response time is limited;

3. nonstandard control effectors and configurations may be required; and

4. the handling/ride qualities of the reconfigured aircraft may be degraded.

The assumptions that failures (or combinations of failures) are not anticipated and that limited time is available for reconfiguration imply that the reconfiguration procedure must be on-line and highly automated. The ability to

use nonstandard control surfaces gives the control system additional degrees of freedom to compensate for the loss of failed surfaces. Despite the additional freedom, the loss of primary control surfaces reduces the performance that the control system can achieve. However, in an emergency situation the first objective is to maintain the aircraft in a stable, flyable state. Any additional handling qualities that can be attained beyond this are desirable but secondary objectives. The combination of non-standard control surfaces with limited performance objectives, and the inherently asymmetric failure effects, will most likely lead to nonstandard control system designs.

1.2 A STRUCTURE FOR RESTRUCTURABLE CONTROL SYSTEMS

The complete problem of designing a restructurable control system can be viewed as three distinct but interrelated problems. This problem structure can be used to define a corresponding candidate structure for restructable control systems as illustrated in Fig. 1-1. The first operation uses a failure detection and identification (FDI) algorithm to detect failed surfaces and identify key parameters. This information is then used to determine a flight condition or operating point for the aircraft.

The outputs of this function are the nominal values of the control surfaces and a corresponding linearized model of the aircraft dynamics. The third function trims, stabilizes and regulates the aircraft within the linear operating region of the specified flight condition.

Although the hierarchy of Fig. 1-1 can be regarded as operating sequentially, it is likely that the most effective implementation will have dynamic interactions between the levels. The FDI algorithm can continue to perform and refine its outputs during and following the operation of the lower two

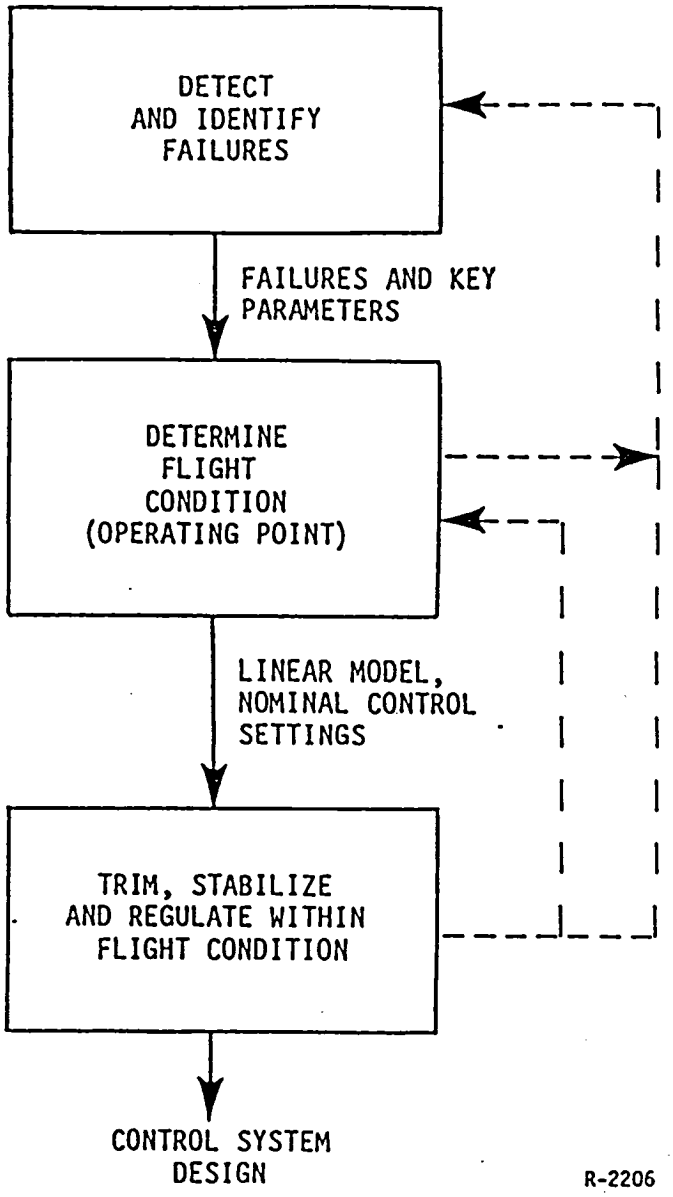

Figure 1-1. Structure for Restructable Control Systems

levels. The choice of flight conditions can be modified as new failure and parameter information arrives or if it is determined that the flight condition cannot be maintained by the linear regulator with the available control authority. The choice of flight condition and linear regulator also impact the performance of the FDI algorithm. These feedback interactions are represented in Fig. 1-1 by dashed lines.

Clearly the development of a comprehensive restructurable control system is a complex problem. Although the functions and interactions indicated by Fig. 1-1 are essential to the operation of the restructurable control system, a reasonable approach to the development of such a system is to first consider each of the levels separately. Once the functions at each level are understood and developed, the results can be combined into a comprehensive system.

The focus of the research presented in this report is the lowest level of the hierarchy in Fig. 1-1: the development of an automatic procedure for designing a linear trim and regulation system. The main emphasis will be placed on the automatic regulator design, however, the formulation of a linear trim system also will be discussed. Each of these procedures must address a multivariable control problem. Although the topic of multivariable control has been studied for many years and numerous approaches to multivariable control system design have been developed [5], none of the design methods can be described as automatic. Typically, good designs still require good engineering judgement applied with an efficient design procedure. Thus the development of an automatic design procedure must translate "good engineering judgment" into design rules that can be applied automatically. The difficulty of this task is lessened by the relaxed performance demands that are present in the restructurable control problem.

1.3 SUMMARY OF THE AUTOMATIC REDESIGN PROCEDURE

The most significant contribution of this report is the development and preliminary analysis of a simple, reliable automatic redesign procedure for restructurable control. This procedure is based on Linear Quadratic (LQ) design methodologies. It employs a robust control system design for the unfailed aircraft to minimize the effects of failed surfaces and to extend the time available for restructuring the FCS. The procedure uses the LQ design parameters for the unfailed system as a basis for choosing the design parameters of the failed system. This philosophy allows the engineering trade-offs that were present in the nominal design to be inherited by the restructurable design. In particular, it allows bandwidth limitations and performance trade-offs to be incorporated in the redesigned system.

The procedure also has several other desirable features. It effectively redistributes authority among the available control effectors to maximize the system performance subject to actuator limitations and constraints. It provides a graceful performance degradation as the amount of control authority lessens. When given the parameters of the unfailed aircraft, the automatic redesign procedure reproduces the nominal control system design. The procedure can incorporate the uncertainty of the aircraft control and stability derivatives that may arise from the use of nonstandard control configurations or from estimates of these derivatives supplied by the FDI algorithm. Finally, the automatic redesign procedure is conceptually simple, easily implemented, and computationally fast.

1.4 OUTLINE

The remainder of this report is divided into five sections. Section 2 discusses the formulation of the linear trim problem and an approach to its solution. Section 3 presents the automatic design procedure and discusses its theoretical interpretations. The performance of the automatic design procedure is demonstrated on a transport class aircraft (a Boeing 737 model) in Section 4, and on a fighter class aircraft in Section 5. The results of the research and recommendations for future research are summarized in Section 6.

1.5 LIST OF SYMBOLS AND NOTATION

d_L ≡ limit vector

d_{LS} ≡ left stabilizer command

d_{RS} ≡ right stabilizer command

j ≡ $\sqrt{-1}$

m ≡ dimension of the input

n ≡ dimension of the system state

n_a ≡ dimension of the aircraft state

n_c ≡ dimension of the compensator state

p ≡ roll rate

q ≡ pitch rate

r ≡ yaw rate

s ≡ complex frequency

u ≡ input

$\bar{u}$ ≡ forward velocity of the aircraft

u_o ≡ linear trim solution

u_i ≡ left singular vectors

u_s ≡ input vector for system with stabilizer dynamics

$\bar{v}$ ≡ side velocity of the aircraft

v_i ≡ eigenvectors

v_{s1}, v_{s2} ≡ right eigenvector for the stabilizer poles

$\hat{v}_{s1}, \hat{v}_{s2}$ ≡ portions of right eigenvectors for the stabilizer poles

w ≡ disturbance

$\bar{w}$ ≡ vertical velocity of the aircraft

x ≡ system state

x_o ≡ linear trim state solution

x_a ≡ aircraft state

x_c ≡ compensator state

x_I ≡ integrator state

x_s ≡ combined aircraft and stabilizer states

y ≡ variables to be regulated

A ≡ system dynamics matrix

$\bar{A}$ ≡ system matrix with reflected eigenvalues

A_a ≡ aircraft dynamics matrix

A_c ≡ compensator dynamics matrix

A_{ca} ≡ compensator-aircraft state matrix

A_s ≡ combined aircraft and stabilizer dynamics matrix

B ≡ system input matrix

$\bar{B}$ ≡ true input matrix

B_a ≡ aircraft input matrix

B_c ≡ compensator input matrix

B_s ≡ combined aircraft and stabilizer input matrix

ΔB ≡ error between true and system input matrix

C ≡ output matrix

C_a ≡ aircraft output matrix

D ≡ design return difference matrix

$\bar{D}$ ≡ true return difference matrix

E ≡ disturbance matrix

F ≡ state limit matrix

G ≡ state feedback matrix

H ≡ input limit matrix

J ≡ quadratic cost functional

I ≡ identity matrix

K ≡ regulator Riccati equation solution

L ≡ loop transfer function

L_c ≡ transfer function from input to state weighting

M ≡ square root of state penalty matrix

$\tilde{M}$ ≡ scaling matrix for adjusting singular values

M_I ≡ square root of the integrator weighting matrix

M_1, M_2, M_3, M_4 ≡ square roots of state weighting matrices for designs 1 through 4

M', M'' ≡ columns of square root of state weighting matrix chosen to retain stabilizer poles

N ≡ square root of input penalty matrix

N_0 ≡ square root of the nominal input penalty matrix

P ≡ bandwidth normalization matrix

Q ≡ state penalty matrix

Q_0 ≡ state penalty matrix for the nominal design

Q_1, Q_2, Q_3, Q_4 ≡ state penalty matrices for designs 1 through 4

Q_d ≡ trim state penalty matrix

R ≡ input penalty matrix

R_0 ≡ input penalty matrix for the nominal design

R_d ≡ trim input/output penalty matrix

S ≡ sensitivity transfer function

$U, \hat{U}$ ≡ matrices of left singular vectors

V ≡ matrix of right singular vectors

$\overline{V}$ ≡ matrix of right eigenvectors

$\overline{V}_s$ ≡ matrix of right eigenvectors of left half plane eigenvalues

$\overline{V}_u$ ≡ matrix of right eigenvectors of right half plane eigenvalues

W ≡ transformed expected effectiveness matrix

$\overline{W}$ ≡ matrix of left eigenvectors

W_o ≡ observability Grammian

W_{co} ≡ controllability-observability Grammian

$\overline{W}_s$ ≡ matrix of left eigenvectors of left half plane eigenvalues

$\overline{W}_u$ ≡ matrix of left eigenvectors of right half plane eigenvalues

W_u ≡ control effectiveness uncertainty matrix

Y ≡ transformed optimization variables

$\beta_{ijk\ell}$ ≡ covariance between the (i,j) and (k,ℓ) elements of the input matrix error

δ_{LT} ≡ left engine thrust

δ_{RT} ≡ right engine thrust

δ_{LS} ≡ left stabilizer

δ_{RS} ≡ right stabilizer

δ_R ≡ rudder

δ_{LE} ≡ left elevator

δ_{RE} ≡ right elevator

δ_{LA} ≡ left aileron

δRA ≡ right aileron

θ ≡ pitch angle

ρ ≡ scaling for input penalty matrix

$\sigma, \hat{\sigma}$ ≡ singular values

τ_s ≡ stabilizer time constant

ϕ ≡ roll angle

ω ≡ frequency

ω_c ≡ bandwidth constraint (crossover) frequency

Λ_s ≡ diagonal matrix of left half plane eigenvalues

Λ_u ≡ diagonal matrix of right half plane eigenvalues

Σ ≡ diagonal matrix of singular values

1.5.2 Functions

A^T ≡ transpose of the matrix A

A^H ≡ complex conjugate of the transpose of the matrix A

e^A ≡ matrix exponential of A

$E\{\cdot\}$ ≡ expected value

λ_{min} ≡ minimum eigenvalue of the indicated matrix

SECTION 2

AN APPROACH TO THE AUTOMATIC DESIGN OF A LINEAR TRIM SYSTEM

2.1 INTRODUCTION

This section presents the formulation and formal solution of a linear trim problem. A linear trim system (i.e., a system that trims the aircraft within the given flight condition) is needed because a control effector failure such as a stuck surface (c.f. [2]) can create a constant force or moment disturbance that must be accommodated within the chosen flight condition. This accommodation can be handled either in the regulator system through the use of integral control or, if the disturbance can be measured, in a linear trim subsystem through the use of feedforward control. The latter approach has the advantages of rapid response to disturbances and of not adversely affecting the stability of the system. Its disadvantage is that any errors between the measured and true disturbance will appear directly in the output.

2.2 THE DISTURBANCE REJECTION PROBLEM

Assume that the linearized model of the aircraft at the chosen flight condition is given by:

$$\dot{x}(t) = Ax(t) + Bu(t) + Ew \qquad (2\text{-}1)$$

where $x(t)$ is the state vector of the linearized aircraft dynamics, $u(t)$ is the vector of available control surfaces (i.e., failed surfaces are deleted) and w is a vector of constant disturbances.

The vector w can be used to represent forces and moments generated by failed surfaces. Examples include the rolling moment caused by the engine loss in the AA DC-10 incident [1] and the pitching and rolling moments induced by the left elevator in the Delta L-1011 incident [2]. This disturbance vector may either be measured (e.g., an identified rolling moment supplied by the FDI algorithm) or unmeasurable.

The objectives of the linear control system designed for the linearized model (2-1) are, in order of priority:

1. stabilize the system;
2. reduce or eliminate the effects of the disturbance vector w on key state variables; and
3. achieve desirable flying qualities.

That is, the primary objective is to produce a control system that achieves a stable, wings level, constant altitude flight. The secondary objective is to enhance the performance of the failed aircraft. This objective will only be considered applicable after the first objective is achieved. The thrust of this research assumes that the failure of the aircraft is such that the first objective can be achieved with the remaining control surfaces. The problems of stabilizing and achieving desirable flying qualities will be addressed by the automatic design procedure developed in Section 3. The problem of steady state disturbance rejection will be formulated in this subsection and a feedforward control solution for measured disturbances will be presented in subsection 2.3.

Let the key states that are to be regulated be denoted by:

$$y = Cx \tag{2-2}$$

Typically, the elements of y would represent states such as the altitude and

bank angle of the aircraft. The objective of our problem will be to automatically design the control system to guarantee that the system is stable, that

$$y = 0, \tag{2-3}$$

and to achieve as much performance as possible.

Two different situations are of interest:

1. a measurement of the disturbance w is available; and
2. the disturbance w is unmeasurable.

In the first case, the disturbance measurement can be fed forward by the control system to mitigate the effects of the disturbance on the variable y. In the second case, the effects of the disturbances can be eliminated by incorporating integral feedback in the compensation. The advantages of feedforward compensation are that it is fast and it does not adversely affect the stability of the system. The disadvantage is that any error in the measurement of the disturbance will show up in the output. The use of integral control will guarantee that the variables y will be driven to zero. However, the response will be slower than that of an equivalent feedforward system, and the integrators make the stabilization problem more difficult. In general, if disturbance measurements are available, it is desirable to incorporate both feedforward and integral feedback in the control system design.

This report will address both feedback structures to some extent. The feedforward problem will be formulated and its solution will be briefly discussed. Since this problem involves an open loop control structure, the only major automatic design issues relate to the on-line solution of the problem. The regulator problem with integral feedback will be discussed in Section 3.

2.3 DISTURBANCE REJECTION WITH MEASURED DISTURBANCES

In this subsection, we assume that some or all of the disturbances w affecting the system (2-1) can be measured. The measurements can be used directly to minimize the effect of the disturbances on the important states (2-2).

In general, there are three important components to the formulation of this problem. The principal objective is to maintain stable flight with certain specified states (2-2) set to zero (2-3). Stable flight implies that the state derivative be zero:

$$0 = Ax + Bu + Ew \tag{2-4}$$

In addition to (2-3) and (2-4), there will be constraints on the magnitudes of the control surfaces and states. We represent these constraints using a linear inequality:

$$Fx + Hu \leq d_L \tag{2-5}$$

Given the objectives (2-3)-(2-5), there may or may not be a set of states x_o and control surfaces u_o that satisfy all three. If a pair (x_o, u_o) satisfying (2-3)-(2-5) do exist, there will generally be more than one such pair. In this case, we will try to choose the pair of least norm:

Feasible Disturbance Rejection Problem

$$\text{minimize} \quad x_o^T Q_d x_o + u_o^T R_d u_o \tag{2-6}$$

$$\text{subject to} \quad 0 = Ax_o + Bu_o + Ew \tag{2-7}$$

$$0 = Cx_o \tag{2-8}$$

$$Fx_o + Hu_o \leq d_L \tag{2-9}$$

Several comments are in order. First, the objective (2-6) attempts to keep the disturbed state and resulting control surface deflections as small as possible. The weightings Q_d and R_d can be used to specify the relative importance of states and controls. These choices can be made off-line based on the physical characteristics of the aircraft and its control surfaces.

Secondly, it should be noted that if a solution to (2-6)-(2-9) exists, it guarantees that the principal objectives (2-7)-(2-9) have been satisfied. That is, the important states can be zeroed (2-8), stable flight is possible (2-7), and no prespecified state or control constraints have been violated (2-9).

Finally, it should be noted that (2-6)-(2-9) must be solved on-line after the disturbance w has been measured. However, (2-6)-(2-9) is a standard quadratic programming problem for which a number of fast, efficient solution algorithms have been developed. If (2-9) is not present, (2-6)-(2-8) is simply a least squares problem whose solution can be found by:

$$\begin{bmatrix} x_o \\ u_o \end{bmatrix} = \begin{bmatrix} A & B \\ C & 0 \end{bmatrix} \# \begin{bmatrix} E \\ 0 \end{bmatrix} w \qquad (2\text{-}10)$$

where # denotes the Moore-Penrose pseudo-inverse (see [6] for details).

It is possible that (2-7)-(2-9) overspecify the problem. In this case, it is impossible to achieve the objectives of the restructurable control problem at the chosen flight condition. However, a variation of (2-6)-(2-9) can be used to gain time to choose a new nominal flight condition or to achieve a slowly degrading flight. The key is to try to minimize the size of both the key state variables and the state derivatives:

Infeasible Disturbance Rejection Problem

minimize

$$[Ax_o + Bu_o + Ew]^T Q_d [Ax_o + Bu_o + Ew] + [Cx_o]^T R_d [Cx_o] \qquad (2\text{-}11)$$

subject to

$$Fx_o + Hu_o \leq d_L \qquad (2\text{-}12)$$

The objective (2-11) attempts to keep the size of the state derivative and key state variables small. The weightings Q_d and R_d can be chosen off-line to reflect the relative importance of the state derivatives and key states. A solution to (2-11)-(2-12) will exist as long as the state and control constraints (2-12) have a non-empty solution set.

As with (2-6)-(2-9), the preceding formulation (2-11)-(2-12) is a quadratic programming problem that can be easily solved on-line using existing algorithms. If (2-12) is not present, then the solution is also given by 2-10).

SECTION 3

THE AUTOMATIC REDESIGN PROCEDURE

3.1 STATE MODEL AND LINEAR QUADRATIC REGULATOR

The purpose of this subsection is to present the problem formulation that forms the basis for the automatic redesign procedure. Let the open loop linearized aircraft dynamics be described in state variable form as:

$$\dot{x}_a(t) = A_a\, x_a(t) + B_a\, u(t) \tag{3-1}$$

where $x_a(t) \in R^{n_a}$ is the aircraft state and $u(t) \in R^m$ is the vector of control effectors available in the unfailed aircraft. Let the key output variables $y(t)$ be given by

$$y(t) = C_a\, x_a(t) \tag{3-2}$$

where $y(t) \in R^p$ with $p \leq$ rank (B). Let any compensator dynamics (e.g., integral, lead, and lag elements) also be represented in state variable form as:

$$\dot{x}_c(t) = A_c\, x_c(t) + A_{ca}\, x_a(t) + B_c\, u(t) \tag{3-3}$$

where $x_c(t) \in R^{n_c}$ is the compensator state vector. In particular, (3-3) can represent the integral control required to eliminate constant disturbances of the form considered in Section 2.

The entire system can then be represented in state form as

$$\dot{x}(t) = Ax(t) + Bu(t) \tag{3-4}$$

$$y(t) = Cx(t) \tag{3-5}$$

where

$$A = \begin{bmatrix} A_c & A_{ca} \\ 0 & A_a \end{bmatrix} \tag{3-6}$$

$$B = \begin{bmatrix} B_c \\ B_a \end{bmatrix} \tag{3-7}$$

$$C = \begin{bmatrix} 0 & C_a \end{bmatrix} \tag{3-8}$$

Linear-Quadratic (LQ) design methodology will be used as the basis for the restructuring algorithm. The LQ regulator problem can be stated as follows. Find the control u(t) that minimizes:

$$J = \int_0^\infty [\, x^T Qx + u^T Ru \,]\, dt \tag{3-9}$$

The optimal control that minimizes (3-9) is given by

$$u(t) = -R^{-1} B^T K\, x(t) \triangleq -G\, x(t) \tag{3-10}$$

where K solves the algebraic Riccati equation

$$0 = A^T K + KA + Q - K B R^{-1} B^T K \tag{3-11}$$

Assuming that the linearized model is valid and that integral control is used, the feedback law (3-10) guarantees that the linearized closed loop system will be stable, and that the important states (3-2) will approach zero regardless of the value of the disturbances. Thus the primary goals of

stability and disturbance rejection will be met by any LQ regulator design. However, certain performance limitations (such as control surface bandwidth) and secondary performance objectives must also be considered.

3.2 FREQUENCY DOMAIN PERFORMANCE SPECIFICATION

Many performance issues are most readily discussed in terms of the sensitivity function (i.e., the inverse of the return difference) of the closed loop system evaluated at the plant inputs:

$$S(s) = [I + G\,(sI-A)^{-1}\,B]^{-1} \tag{3-12}$$

The relationship of S to feedback system performance has been discussed extensively in the literature (c.f. [7]-[10]). In general, one obtains benefits from feedback at those frequencies for which

$$\| S(j\omega) \| < 1 \tag{3-13}$$

The benefits include improved response due to dynamic input disturbances and a reduction of the effects of parameter variation. The frequency range over which (3-13) can be achieved is generally limited by the dynamic uncertainty of the plant, sensors, and actuators. As a result of these uncertainties, the loop transfer function

$$L(s) = G\,(sI - A)^{-1}\,B \tag{3-14}$$

must be rolled off before the uncertainties become significant.

The sensitivity function of a LQ regulator possesses special properties. It satisfies the Kalman equality [11]:

$$S(-s)^{-T}\,R\,S(s)^{-1} = R + B^{T}\,(-sI-A)^{-T}\,Q(sI-A)^{-1}B \tag{3-15}$$

Equation (3-15) expresses the return difference of the closed loop system in terms of the open loop system and the penalty matrices Q and R. Thus the performance of the closed loop system can be determined analytically in terms of the LQ design parameters. This point will be exploited in the automatic design procedure described in the sequel.

Equation (3-15) is often more conveniently viewed in a slightly modified form. Let N denote the inverse of the square root of R, i.e.

$$R = N^{-T}N^{-1} \tag{3-16}$$

Pre- and post-multiplying (3-15) by N^T and N respectively gives:

$$[N^T S(-s)^{-T} N^{-T}] [N^{-1} S(s)^{-1}N] = I + N^TB^T (-sI-A)^{-T} Q(sI-A)^{-1} BN \tag{3-17}$$

The left side of (3-17) is a quadratic form that represents the size of the closed loop return difference as weighted by the input penalty matrix. This weighting normalizes the return difference with respect to the relative importance of the controls. The right hand side is the sum of a positive semi-definite definite matrix and the identity. Consequently, the weighted return difference is always greater than unity. The amount by which it exceeds unity (and hence the amount of beneficial feedback) is determined explicitly and analytically by Q and N (equivalently R).

The bandwidth limitations on the loop transfer function L(s) (3-14) can be imposed by unmodeled plant, sensor, or actuator dynamics. We will assume that these constraints can be expressed in terms of a constraint on the norm of the loop transfer function at the input of the closed loop plant of the following form:

$$\| PL(j\omega_c) \| < 1 \qquad (3\text{-}18)$$

In condition (3-18), ω_c represents a critical frequency at which the bandwidth constraints are imposed. Since the loops of a multivariable system may have different bandwidths, the weighting matrix P is used to indicate the relative size of the control loops at the critical frequency. In effect, the matrix P can be regarded as scaling the input matrix for analysis purposes. For example, suppose that in a two input system, one actuator has a bandwidth limit of 1 rad/sec while the second actuator has a bandwidth limit of 10 rad/sec. These restrictions can be incorporated in a single constraint of the form of (3-18) by specifying

$$\omega_c = 10 \text{ rad/sec}$$

$$P = \begin{bmatrix} 10 & 0 \\ 0 & 1 \end{bmatrix}$$

Note that the choice of $P_{11} = 10$ implies the first loop will be at most -20dB when the second loop crosses over. Since a LQ regulator rolls off at a rate of 20dB/decade, the 1 rad/sec bandwidth limit on the first loop will be enforced.

The constraint (3-18) uses the control loop gain G explicitly. Since the gain G is related to the LQ design parameters Q and R in a complex, nonlinear manner, it is desirable to approximate (3-18) with a constraint that employs Q and R explicitly. Fortunately, a simple approximation to (3-18) can be obtained from the Kalman Equality (3-17).

The attempt to ensure that the loop transfer function is small (i.e., condition (3-18)) can be roughly approximated by trying to keep the return difference small (i.e., near unity). The latter can be accomplished by controlling

the size of the right hand side of (3-17). Note that the right side of (3-17) can be written as

$$I + L_c(-s)^T L_c(s) \tag{3-19}$$

where

$$L_c(s) = M (sI - A)^{-1} BN \tag{3-20}$$

and M is a m×m square root of Q:

$$Q = M^T M$$

Thus, we can approximately impose (3-18) by using the transfer function $L_c(s)$ in (3-18) rather the true transfer function L(s). That is, we can replace (3-18) by:

$$\| PM(j\omega_c I - A)^{-1} BN \| < 1 \tag{3-21}$$

Thus, (3-21) approximately represents the bandwidth limitations and is expressed only in terms of open loop and design quantities.

3.3 DEVELOPMENT OF THE AUTOMATIC REDESIGN PROCEDURE

3.3.1 Formulation as an Optimization Problem

Given a failure of one or more aircraft control surfaces, the objective of the linear restructurable control system is to redesign the linear control law in a manner that preserves as much of the aircraft safety and performance as possible. Clearly, the primary objective is to stabilize the aircraft. Assuming that this is possible for the given flight condition and available actuator power and bandwidth, the secondary but still important objective of maintaining aircraft performance can then be considered. This objective can

be translated into the control system objective of maximizing the amount of beneficial feedback in order both to maximize robustness due to uncertain system parameters and to minimize disturbance effects.

The preceding considerations form the basis for the linear restructuring algorithm developed in this section. The automatic redesign procedure will use LQ regulator designs for the restructured FCS. Thus the design parameters to be chosen by the automatic redesign procedure are the quadratic penalty matrices Q and R.

We will assume that a nominal LQ design for the unfailed aircraft is available. The design can be characterized by the quadratic weights Q_o and R_o that were used to develop the nominal design. The automatic redesign procedure exploits the engineering trade-offs that were made in the choice of Q_o and R_o for the unfailed aircraft by fixing

$$Q = Q_o \tag{3-22}$$

and choosing a new value for R. The choice of Q as in (3-22) ensures that the relative importance of each state (or combination of states) is maintained in the Linear Quadratic regulator problem for the failed aircraft design, thereby incorporating the physical engineering trade-offs from the unfailed FCS design in the restructured design.

The design parameter that will be specified by the automatic redesign procedure is the input penalty matrix R. The formal objective of the the automatic design procedures will be to choose R to maximize performance in an appropriate sense while satisfying the bandwidth constraints (3-18). Specifically, we pose the problem:

$$\underset{N\in R^{mxm}}{\text{maximize}} \quad \lambda_{min}\left\{ \int_{-\infty}^{\infty} [N^T B^T(-j\omega I-A)^{-T} Q (j\omega I - A)^{-1} BN]\, d\omega \right\} \qquad (3\text{-}23)$$

subject to

$$\| PG (j\omega_c I - A)^{-1} B \| < 1 \qquad (3\text{-}24)$$

The objective (3-23) is simply to maximize the smallest eigenvalue of the frequency integral of the right hand side of (3-17). Consequently, this objective expresses the desire to maximize in an integral sense the performance of the closed loop system.

The bandwidth constraint (3-24) can be simplified by replacing it with the approximation (3-21) that was developed in subsection 3.2. This approximation can be further simplified by assuming that R_o satisfies (3-21). Let

$$R_o^{-1} = N_o N_o^T \qquad (3\text{-}25)$$

If N_o satisfies (3-25), the constraint

$$\| N_o^{-1} N \| < 1 \qquad (3\text{-}26)$$

guarantees that (3-21) will also be satisfied. Hence (3-26) can be used to approximate the bandwidth constraint (3-24). A procedure for choosing N following a failure will be developed in subsections 3.3.2 and 3.3.3.

The objective function (3-23) can also be simplified. If A is a strictly stable matrix, the application of Parseval's theorem to (3-23) yields the equivalent objective:

$$\underset{N\in R^{mxm}}{\text{maximize}} \; 2\pi \cdot \lambda_{min} \{N^T B^T \int_o^{\infty} e^{A^T t} Q_o e^{At}\, dt\, BN\} \qquad (3\text{-}27)$$

The integral in (3-27) is simply the infinite horizon observability Grammian associated with the quadratic cost (3-9). It can be evaluated as the solution to the Lyapunov equation:

$$A^T W_o + W_o A + Q_o = 0 \tag{3-28}$$

The objective (3-27) then becomes

$$\underset{N \in R^{mxm}}{\text{maximize}} \quad 2\pi \cdot \lambda_{min} \{N^T B^T W_o B N\} \tag{3-29}$$

Objective (3-29) has a nice interpretation in terms of the effectiveness of control on the important state variables. Recall that it was assumed that Q_o has been chosen to reflect the relative importance of the various state variables to the performance of the aircraft. The matrix $B^T W_o B$ then reflects the amount of energy that can be transmitted to those variables, weighted by their perceived importance, from each of the available control surfaces. Hence (3-29) captures the issue of quantifying control effectiveness.

If A is a strictly unstable matrix (i.e., all eigenvalues of A are in the open right half plane), the application of Parseval's relation to (3-23) yields a result analogous to (3-27), but with -A replacing A. Relations analogous to (3-28)-(3-29) can then be derived. Although we are primarily interested in stable airframes, A could in general have eigenvalues in both the left and right half planes. In this case, relations analogous to (3-27)-(3-28) can still be derived, but the application of Parseval's theorem to (3-23) must incorporate a spectral factorization of the integrand.

Specifically, assume that the system matrix has the spectral decomposition:

$$A = \begin{bmatrix} \bar{W}^H_s & \bar{W}^H_u \end{bmatrix} \begin{bmatrix} \Lambda_s & 0 \\ 0 & \Lambda_u \end{bmatrix} \begin{bmatrix} \bar{V}_s \\ \bar{V}_u \end{bmatrix} \tag{3-30}$$

where Λ_s is a diagonal matrix with its diagonal elements being the open left half plane eigenvalues of A, and Λ_u is a diagonal matrix with its diagonal elements being the open right half plane eigenvalue of A. We will assume that any eigenvalues of A on the $j\omega$ axis have been shifted by a small factor ε into the left half plane. Define

$$\bar{A} = \begin{bmatrix} \bar{W}_s^H & \bar{W}_u^H \end{bmatrix} \begin{bmatrix} \Lambda_s & 0 \\ 0 & -\Lambda_u \end{bmatrix} \begin{bmatrix} \bar{V}_s \\ \bar{V}_u \end{bmatrix} \tag{3-31}$$

Then (3-27)-(3-29) are correct with $\bar{A}$ replacing A. For computational purposes, $\bar{W}$ and $\bar{V}$ in (3-30)-(3-31) can be replaced by any matrices that effect a decomposition of A into its stable and unstable invariant subspaces. These matrices can be computed efficiently and accurately [12].

Thus, the problem considered by the automatic design procedure is:

$$\underset{N \in R^{m \times m}}{\text{maximize}} \quad 2\pi \lambda_{min} \{N^T W_{co} N\} \tag{3-32}$$

subject to

$$\| N_o^{-1} N \| < 1 \tag{3-33}$$

where

$$W_{co} = B^T W_o B \tag{3-34}$$

$$A^T W_o + W_o A + Q = 0 \tag{3-35}$$

3.3.2 Solution of the Automatic Redesign Problem Without Uncertainty

The solution of (3-32)-(3-35) is almost trivial. Since

$$W_o > 0 \tag{3-36}$$

the objective functional (3-32) is also positive for any choice of N, and is monotonicly nondecreasing as N increases in size. Thus N should be chosen as large as possible. The only constraint on N is the bandwidth constraint (3.33). Hence, the choice

$$N = N_o \tag{3-37}$$

solves the restructuring problem formulated in subsection 3.3.1.

Thus, in the case when information about control effector uncertainty is not used by the automatic redesign procedure, the procedure simply solves a LQ regulator problem with the new system description supplied by the FDI algorithm and the nominal design quadratic weights Q_o and R_o. This has the advantage of not requiring any computation to choose the design parameters. Yet, since it is the solution to the problem posed in subsection 3.3.1, the simple procedure effectively maximizes the achievable performance within the bandwidth constraints of the system. A similar approach using output feedback has been used successfully in [14].

3.3.3 The Automatic Redesign Procedure with Surface Uncertainty

The preceding section presented an automatic design algorithm that assumed that the effectiveness of each of the unfailed surfaces is known. However, as noted in Section 1, the use of surfaces in non-standard configuration, and the failure effects themselves, may result in uncertain control effectiveness. Also, the problems due to false alarms in failure detection and isolation algorithms (FDI) can be reduced by incorporating surface uncertainties in the restructuring algorithm. That is, an FDI algorithm can supply certainty estimates for surfaces that may or may not have failed. The purpose of this section is to modify the automatic design procedure described in subsections 3.3.1 through 3.3.2 to incorporate estimates of uncertainty in the surface effectiveness.

The nominal control surface effectivenesses are determined by the input matrix B. We will assume that the true effectivenesses are given by $\overline{B}$ and that

$$\overline{B} = B + \Delta B \tag{3-38}$$

where ΔB represents the uncertainty in the effectiveness. We will assume that the uncertainty has zero mean:

$$E \{ \Delta B \} = 0 \tag{3-39}$$

and that the covariance between the i,jth element and the (k,ℓ)th element is:

$$E \{ \Delta B_{ij} \Delta B_{k\ell} \} = \beta_{ijk\ell} \tag{3-40}$$

The performance of the true system is determined by the singular values of the return difference:

$$\overline{D}(s) = I + G (sI-A)^{-1} \overline{B} \tag{3-41}$$

The Kalman Equality for the nominal return difference D(s) is:

$$D(-s)^T R D(s) = R + B^T (-sI-A)^{-T} Q (sI-A)^{-1} B \tag{3-42}$$

Using (3-38) and the definition of $\overline{D}(s)$ (3-41) gives

$$\left\{ \begin{array}{l} \overline{D}(-s)^T R \overline{D}(s) - \overline{D}(-s)^T R G (sI-A)^{-1} \Delta B \\ \quad -\Delta B^T (-sI-A)^{-T} G^T R \overline{D}(s) \\ \quad + \Delta B^T (-sI-A)^{-T} G^T RG (sI-A)^{-1} \Delta B \\ \quad = R + B^T (-sI-A)^{-T} Q (sI-A)^{-1} B \end{array} \right. \tag{3-43}$$

To find the average performance of the control system over the range of uncertainty, we take the expected value of both sides of (3-43). Rearranging terms yields:

$$E\{\bar{D}(-s)^T R \bar{D}(s)\} = R + B^T(-sI-A)^{-T} Q (sI-A)^{-1} B - E\{\Delta B^T(-sI-A)^{-T} G^T RG (sI-A)^{-1} \Delta B\} \quad (3-44)$$

The left hand side of (3-44) represents the expected performance of the control system. The right hand side of (3-44) contains the same terms as the Kalman equality minus a term due to the control surface effectiveness uncertainty. Recall that the automatic design procedure was developed to maximize the expected performance by using the frequency integration of the second and third terms of (3-44).

Before performing the integration, we should note that the term due to the control surface uncertainty is already a function of the feedback gain G and thus of the Q and R matrices that are to be chosen. To eliminate this dependency, we can use the approximation

$$G^TRG \approx Q \quad . \quad (3-45)$$

Equation (3-44) then becomes

$$E\{\bar{D}(-s)^T R \bar{D}(s)\} = R + B^T(-sI-A)^{-T} Q (sI-A)^{-1} B - E\{\Delta B^T(-sI-A)^{-T} Q (sI-A)^{-1} \Delta B\} \quad (3-46)$$

Integrating the second and third terms on the right side of (3-46) and using Parseval's theorem (with A modified, if necessary, as in (3-31) yields:

$$B^T W_o B - E\{\Delta B^T W_o \Delta B\} \quad (3-47)$$

where W_o satisfies (3-28). Define

$$W_u = E \{ \Delta B^T W_o \Delta B \} \tag{3-48}$$

Then the (i,j)th element of W_u is:

$$W_{u_{ij}} = \sum_{\ell=1}^{n} \sum_{k=1}^{n} W_{o_{\ell k}} \beta_{ki} \beta_{\ell j} \tag{3-49}$$

Finally, we use the same objective as was used in subsection 3.3.1 to define the modified automatic design algorithm. That is, we attempt to maximize the smallest eigenvalue of $N^T P N$. The optimization problem becomes:

$$\max \lambda_{min} \{ N^T [W_{co} - W_u] N \} \tag{3-50}$$

subject to

$$\| N_o^{-1} N \| \leq 1 \tag{3-51}$$

where W_{co} and W_o are given by

$$W_{co} = B^T W_o B \tag{3-52}$$

$$A^T W_o + W_o A + Q_o = 0 \tag{3-53}$$

and W_u is given by (3-48)-(3-49).

The solution to (3-50)-(3-52) is not quite as easy as the solution presented in subsection 3.3.2. Define

$$Y = N_o^{-1} N \tag{3-54}$$

Then (3-50)-(3-51) become:

$$\max \lambda_{min} \{ Y^T W Y \} \tag{3-55}$$

subject to

$$\| Y \| < 1 \tag{3-56}$$

where

$$W = N_o^{-T} [W_{co} - W_u] N_o^{-1} \tag{3-57}$$

Unlike (3-32), W may not be positive definite due to the uncertainty matrix W_u. Thus simply taking Y to be the identity could result in a negative value for (3-55).

The solution can be obtained in terms of the eigenvectors of W. Let the columns of Y be an orthonormal basis for the invariant subspace (eigenspace) of W corresponding to the non-negative eigenvalues of W. Then Y solves (3-55)-(3-57). The matrix N is given by

$$N = N_o Y \tag{3-58}$$

and the design matrix R is specified by

$$R^{-1} = N N^T \tag{3-59}$$

Since W is the beneficial feedback (W_{co}) minus the uncertainty (W_u), a negative eigenvalue results only if uncertainty exceeds benefit in some direction. This direction is represented by the corresponding eigenvector of W and is eliminated from consideration in the control law design. Hence, the solution eliminates those combinations of controls for which the control uncertainty exceeds the control effectiveness within the feedback design.

The modified automatic design algorithm can be summarized as follows. Once again, it assumes that a nominal LQ design has been chosen with nominal weights Q_o and R_o. It also assumes that an FDI algorithm has indicated either a control surface failure or uncertainty about the operation of a surface.

Modified Automatic Design Algorithm:

Step 0: Pre-compute and store

$$N_o = \left(\sqrt{R_o}\right)^{-1}$$

$$\bar{A} = \begin{bmatrix} \bar{W}_s^H & \bar{W}_u^H \end{bmatrix} \begin{bmatrix} \Lambda_s & 0 \\ 0 & -\Lambda_u \end{bmatrix} \begin{bmatrix} \bar{V}_s \\ \bar{V}_u \end{bmatrix}$$

where

$$A = \begin{bmatrix} \bar{W}_s^H & \bar{W}_u^H \end{bmatrix} \begin{bmatrix} \Lambda_s & 0 \\ 0 & \Lambda_u \end{bmatrix} \begin{bmatrix} \bar{V}_s \\ \bar{V}_u \end{bmatrix}$$

Step 1: Form the matrix B from the unfailed surfaces.

Step 2: Compute W:

$$W = N_o^{-T} \left[W_{co} - W_u \right] N_o^{-1}$$

$$W_{co} = B^T W_o B$$

$$A^T W_o + W_o A + Q_o = 0$$

$$W_{u_{ij}} = \sum_{\ell=1}^{n} \sum_{k=1}^{n} W_{o_{\ell k}} \beta_{ki\ell j}$$

Step 3: Find the eigenvectors $v_1, \ldots, v_\ell$ corresponding to the positive eigenvalues of W. Define

$$N = N_o \left[v_1 \ldots v_\ell \right]$$

Step 4: Compute

$$R^{-1} = N N^T$$

Step 5: Solve the LQ regulator problem

$$A^T K + KA + Q_o - KBR^{-1} B^T K = 0$$

$$G = R^{-1} B^T K$$

SECTION 4

APPLICATION TO A TRANSPORT CLASS AIRCRAFT (BOEING 737 MODEL)

The automatic redesign procedure presented in Section 3 will be demonstrated in this section on a linearized model of a Boeing 737 aircraft. The model is described in subsection 4.1. Subsection 4.2 develops the nominal Linear Quadratic Regulator design for the aircraft. Subsection 4.3 then demonstrates the automatic redesign procedure on this aircraft.

4.1 Aircraft Model

A linearized model of the NASA Boeing 737 aircraft operating at different flight conditions was supplied by NASA to ALPHATECH to demonstrate the automatic design procedure. Since this aircraft has nine independent control surfaces, it is an ideal candidate for control restructuring. For this demonstration, an operating point with velocity of 217.4 feet/sec and an altitude of 1000 feet was chosen.

The linear aircraft model is in the form

$$\dot{x}_a(t) = A_a\, x_a(t) + B_a\, u(t) \qquad (4\text{-}1)$$

where x(t) is a state vector of the linear aircraft dynamics and u(t) is the vector of available control surfaces. The state vector is given by

$$x_a = \{\, \bar{u},\ \bar{w},\ q,\ \theta,\ \bar{v},\ p,\ r,\ \phi \,\}^T \qquad (4\text{-}2)$$

where $\bar{u}$ is the forward velocity, $\bar{w}$ is the vertical velocity, q is the pitch rate, θ is the pitch angle, $\bar{v}$ is the side velocity, p is the roll rate, r is the yaw rate and ϕ is the roll angle. The NASA model included a ninth state for yaw angle which was eliminated since it will not be controlled by the regulation system. The longitudinal dynamics are uncoupled from the lateral dynamics. The first four states represent the longitudinal dynamics and the second four represent the lateral dynamics.

The input vector is given by

$$u = \{ \delta_{LT}, \delta_{RT}, \delta_{LS}, \delta_{RS}, \delta_{R}, \delta_{LE}, \delta_{RE}, \delta_{LA}, \delta_{RA} \}^{T} \qquad (4\text{-}3)$$

where δ_{LT} is the left engine thrust, δ_{RT} is the right engine thrust, δ_{LS} is the left stabilator, δ_{RS} is the right stabilator, δ_{R} is the rudder, δ_{LE} is the left elevator, δ_{RE} is the right elevator, δ_{LA} is the left aileron and δ_{RA} is the right aileron.

The system matrix for this operating condition is given by

$$A_a = \begin{bmatrix} -0.0389 & 0.1002 & -7.171 & -32.163 & 0.0 & 0.0 & 0.0 & 0.0 \\ 0.2784 & -0.720 & 217.3 & 0.6562 & 0.0 & 0.0 & 0.0 & 0.0 \\ -0.00024 & -0.0064 & -0.531 & -0.00033 & 0.0 & 0.0 & 0.0 & 0.0 \\ 0.0 & 0.0 & 1.0 & 0.0 & 0.0 & 0.0 & 0.0 & 0.0 \\ 0.0 & 0.0 & 0.0 & 0.0 & -0.149 & 8.803 & -216.3 & 32.16 \\ 0.0 & 0.0 & 0.0 & 0.0 & -.0170 & -1.560 & 0.8067 & -.000085 \\ 0.0 & 0.0 & 0.0 & 0.0 & 0.0033 & -.1175 & -.1503 & -.00404 \\ 0.0 & 0.0 & 0.0 & 0.0 & 0.0 & 1.0 & -.0194 & 0.0 \end{bmatrix} \qquad (4\text{-}4)$$

The input matrix is given by

$$B_a = \begin{bmatrix} 0.00038 & 0.00038 & 0.00575 & 0.00575 & 0.0 & 0.00276 & 0.00276 & 0.00138 & 0.00138 \\ -.00000024 & -.00000024 & -.174 & -.174 & 0.0 & -.0835 & -.0835 & -.0418 & -.0418 \\ 0.00000626 & 0.00000626 & -.0228 & -.0228 & 0.0 & -.0109 & -.0109 & -.0027 & -.0027 \\ 0.0 & 0.0 & 0.0 & 0.0 & 0.0 & 0.0 & 0.0 & 0.0 & 0.0 \\ 0.0 & 0.0 & 0.0023 & -.0023 & 0.143 & 0.00111 & -.00111 & 0.00056 & -.00056 \\ 0.0000015 & -.0000015 & 0.0044 & -.0044 & 0.0096 & 0.002 & -.002 & 0.0085 & -.0085 \\ 0.000012 & -.000012 & 0.00074 & -.00074 & -.0112 & 0.00035 & -.00035 & 0.00071 & -.00071 \\ 0.0 & 0.0 & 0.0 & 0.0 & 0.0 & 0.0 & 0.0 & 0.0 & 0.0 \end{bmatrix} \quad (4\text{-}5)$$

The open loop eigenvalues of the aircraft are:

Short Period:	$-.63 \pm 1.17j$
Phugoid:	$-.017 \pm .17j$
Dutch Roll:	$-.059 \pm 1.11j$
Spiral:	$-.0073$
Roll Subsidence:	-1.735

4.2 LINEAR QUADRATIC REGULATOR DESIGN

The control design is based on robust linear quadratic (LQ) regular theory [13]. The objective of the quadratic design is to minimize a quadratic performance index in the form

$$J = \int_0^\infty [\, x^T Q\, x \; + u^T R\, u \,]\, dt \quad (4\text{-}6)$$

where Q is the state penalty matrix and R is the control penalty matrix. These two penalty matrices are the LQ design parameters and must be chosen to reflect control effectiveness, control uncertainty and other performance requirements. The optimal control that minimizes u(t) is given by

$$u(t) = -R^{-1}\, B^T\, K\, x(t) = -G\, x(t) \quad (4\text{-}7)$$

where K solves the algebraic Ricatti equation

$$0 = A^T K + K^T A + Q - K B R^{-1} B^T K \tag{4-8}$$

4.2.1 Performance Specifications

Linear quadratic theory guarantees the stability and disturbance rejection properties of the linear closed loop design. The state and control penalty matrices, however, must be carefully chosen to reflect performance limitations such as bandwidth constraints. As noted in Section 3, the performance of multiinput, multioutput (MIMO) systems can be discussed in terms of the sensitivity function. The sensitivity function, or the inverse of the return difference of the closed loop system evaluated at the plant inputs, is given as a function of complex frequency (s) by

$$S(s) = [I + G(sI - A)^{-1} B]^{-1} \tag{4-9}$$

The relationship of S(s) to feedback system performance has been discussed extensively in the literature [7]-[10]. Beneficial feedback is obtained for any frequency for which the sensitivity function is less than unity. Because of the uncertainties in the model at high frequencies, the loop transfer function at the input of the closed loop plant

$$L(s) = G\,(sI - A)^{-1}B \tag{4-10}$$

must be rolled off before the uncertainties become significant. For the Boeing 737 model, the desired crossover of the singular values of loop transfer function was between 1 and 5 rad/sec. The singular values of the return difference should attenuate to between .5 and 2.0 dB at 20.0 rad/sec.

4.2.2 Initial Design

An iterative approach is required to choose the state and control penalty matrix which will reflect the performance specifications. For the initial design an identity matrix was chosen for the control penalty matrix and a simple diagonal structure was chosen for the state penalty matrix. Each diagonal element of the state penalty matrix corresponded to the inverse of the maximum value of the appropriate state squared. The state penalty matrix for the initial design is given by

$$Q_1 = \text{diag} \left(100.0^{-2},\ 20.0^{-2},\ .7^{-2},\ .35^{-2},\ 20.0^{-2},\ .7^{-2}\ .7^{-2}\ .35^{-2} \right) \qquad (4\text{-}11)$$

Several initial designs were performed with different values for the control penalty matrix scale factor, ρ. As ρ increases, the magnitude of the loop transfer function increases. Figs. 4-1 and 4-2 show the singular values of the return difference and the loop transfer function, respectively, for $\rho = .01$. There are two lateral loops. An analysis of the corresponding singular vectors indicated that the primary lateral loop is mainly due to contributions from the rudder to damp the Dutch Roll mode. The other lateral loop is mainly an aileron loop (see Figs. 4-1 and 4-2). The longitudinal loop and the rudder loop have acceptable bandwidth and magnitude. The magnitude and bandwidth of the aileron loop, however, should be increased.

Several attempts were made to increase the magnitude and bandwidth of the aileron lateral loop by scaling the state penalty matrix. A loop transfer function can be approximated by the expression

$$L_c(s) = M_1(sI - A)^{-1}\ BN \qquad (4\text{-}12)$$

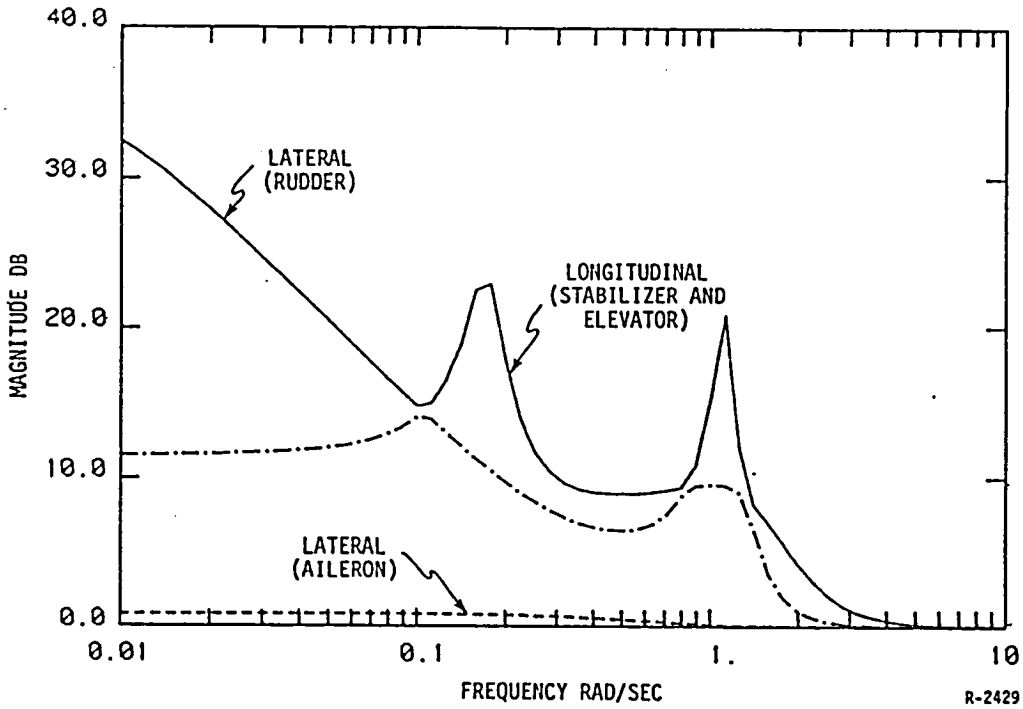

Figure 4-1. Singular Values of Return Difference for Design 1

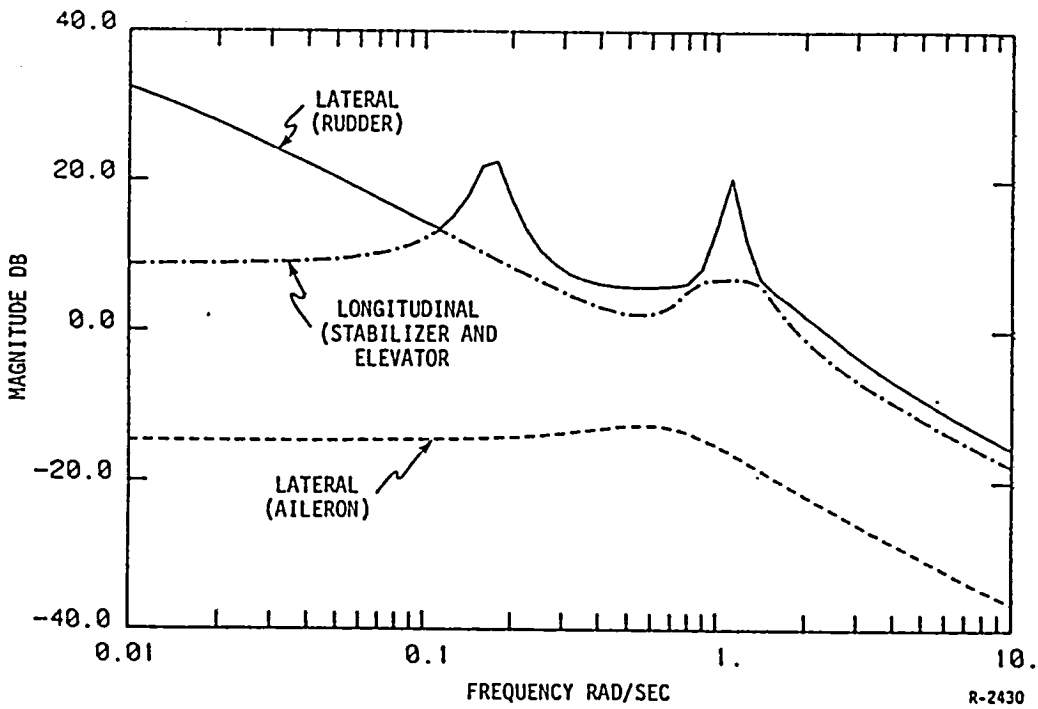

Figure 4-2. Singular Values of Loop Transfer for Design 1

where M_1 is the square root of Q_1 and N is the square root of R^{-1}. At zero frequency (d.c.) this expression becomes

$$L_c(0) = -M_1 \; A^{-1} \; B \; N \tag{4-13}$$

The singular values of the loop transfer function can be moved independently at 0 frequency by an appropriate adjustment of the matrix M. Let the singular value decomposition of $L_c(0)$ be defined by

$$L_c(0) = U \; \Sigma \; V^H$$

Define M as:

$$\hat{M} = D \; U^H$$

where D is a diagonal scaling matrix:

$$D = \begin{bmatrix} d_1 & & 0 \\ & \ddots & \\ 0 & & d_m \end{bmatrix}$$

Then

$$\hat{M} \; L_c(0) = -\left[\hat{M} \; M_1 \right] A^{-1} \; B \; N = D \; \Sigma \; V^H \tag{4-14}$$

has singiular values $\hat{\sigma}_1, \ldots, \hat{\sigma}_m$ where

$$\hat{\sigma}_i = d_i \; \sigma_i$$

and $\{\sigma_1, \ldots, \sigma_m\}$ are the singular values of $L_c(0)$. Thus each singular value at $\omega = 0$ can be chosen independently by an appropriate choice of $\hat{M}$ as in (4-14), and by specifying the new design parameters as:

$$M_2 = \hat{M}\, M$$

$$Q_2 = M_2^T\, M_2$$

A matrix $\hat{M}$ was chosen to move only the aileron loop singular value by choosing $d_3 = 7.62$. The state penalty matrix Q_2 is given by:

$$Q_2 = \left[\begin{array}{cccc|cccc} 0.0001 & 0.0000 & 0.0000 & 0.0000 & 0.0000 & 0.0000 & 0.0000 & 0.0000 \\ 0.0000 & 0.0025 & 0.0000 & 0.0000 & 0.0000 & 0.0000 & 0.0000 & 0.0000 \\ 0.0000 & 0.0000 & 2.0408 & 0.0000 & 0.0000 & 0.0000 & 0.0000 & 0.0000 \\ 0.0000 & 0.0000 & 0.0000 & 8.1633 & 0.0000 & 0.0000 & 0.0000 & 0.0000 \\ \hline 0.0000 & 0.0000 & 0.0000 & 0.0000 & 0.1434 & -0.0015 & -0.0788 & -0.9053 \\ 0.0000 & 0.0000 & 0.0000 & 0.0000 & -0.0015 & 2.0408 & 0.0009 & 0.0098 \\ 0.0000 & 0.0000 & 0.0000 & 0.0000 & -0.0788 & 0.0009 & 2.0849 & 0.5061 \\ 0.0000 & 0.0000 & 0.0000 & 0.0000 & -0.9053 & 0.0098 & 0.5061 & 13.9780 \end{array}\right] \qquad (4\text{-}15)$$

The singular values of the return difference and the loop transfer function are shown in Figs. 4-3 and 4-4 respectively. Note that the d.c. gain of the second lateral loop is now virtually identical to the singular value of the dominant longitudinal loop. Dynamic compensation could be added in a later design to increase the bandwidth of this loop. However, for the purposes of this report (i.e., to demonstrate the redesign algorithm) this additional compensation will not be required.

The closed loop eigenvalues of this design are:

Short Period:	$-1.4 \pm 1.6j$
Phugoid:	$-0.096 \pm .184j$
Dutch Roll:	$-2.0 \pm 2.3j$
Roll Subsidence:	-1.78
Spiral:	$-.25$

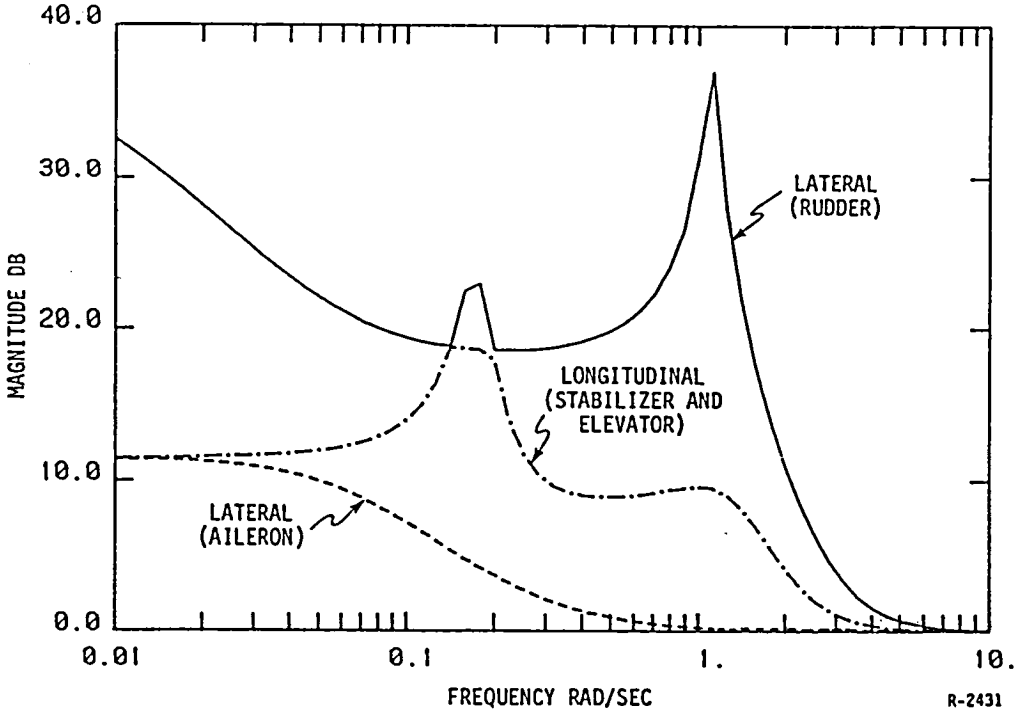

Figure 4-3. Singular Values of Return Difference for Design 2

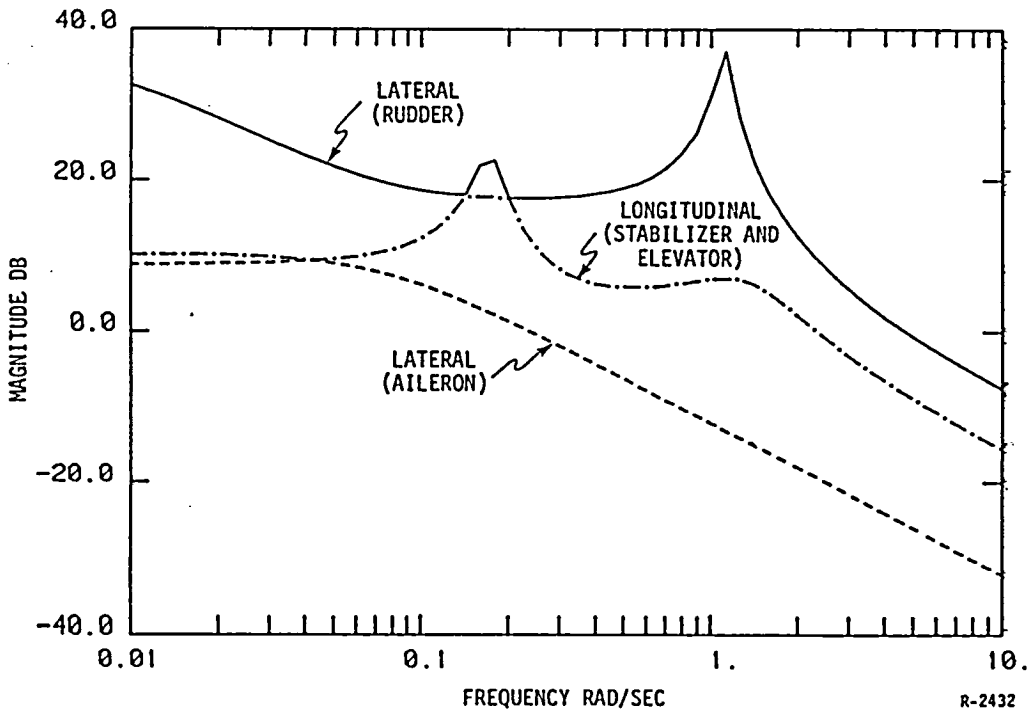

Figure 4-4. Singular Values of Loop Transfer for Design 2

4.2.3 Bandwidth Limits on the Stabilizers

Since the response time of the stabilizers is limited, it is necessary to incorporate bandwidth limits into the LQ design. To add dynamic compensation, the state is augmented with the stabilizer angles to form a new state vector

$$x_S = \{ \bar{u}\ \bar{w}\ q\ \theta\ \bar{v}\ p\ r\ \phi\ \delta_{LS}\ \delta_{RS} \}^T \tag{4-16}$$

and the new input vector includes the drive signals to the stabilator actuators (d_{LS},d_{RS})

$$u_S = \{ \delta_{LT},\ \delta_{RT},\ d_{LS},\ d_{RS},\ \delta_R,\ \delta_{LE},\ \delta_{RE},\ \delta_{LA},\ \delta_{RA} \}^T \tag{4-17}$$

The corresponding augmented system matrix, A_S, and input matrix B_S, are

$$A_S = \left[\begin{array}{c|cc} A_a & B_3 & B_4 \\ \hline 0 & -1/\tau_s & 0 \\ & 0 & -1/\tau_s \end{array}\right] \tag{4-18}$$

and

$$B_S = \left[\begin{array}{cc|cc|ccccc} B_1 & B_2 & 0 & 0 & B_5 & B_6 & B_7 & B_8 & B_9 \\ \hline 0 & & 1/\tau_s & 0 & & & 0 & & \\ & & 0 & 1/\tau_s & & & & & \end{array}\right] \tag{4-19}$$

where $-1/\tau_s$ is the stabilator pole and B_j is the jth column of the input matrix B_a.

To design an effective controller for this augmented system, a state penalty matrix which will not affect the stabilator poles at $-1/\tau_s$ must be

chosen. For the augmented system the state penalty matrix can be defined as

$$Q_3 = M_3^T M_3 \tag{4-20}$$

$$M_3 = [\, M_2 \; M' \; M'' \,] \tag{4-21}$$

and M' and M'' ε $R^{n\times 1}$. The right eigenvectors for the stabilator poles are defined as

$$v_{s1} = \begin{bmatrix} \hat{v}_{s1} \\ 1 \\ 0 \end{bmatrix} \tag{4-22}$$

and

$$v_{s2} = \begin{bmatrix} \hat{v}_{s2} \\ 0 \\ 1 \end{bmatrix} \tag{4-23}$$

Therefore

$$\left[\begin{array}{c|c|c} A_a & B_3 & B_4 \\ \hline 0 & -1/\tau_s & 0 \\ & 0 & -1/\tau_s \end{array}\right] \begin{bmatrix} \hat{v}_{s1} \\ 1 \\ 0 \end{bmatrix} = -\frac{1}{\tau_s} \begin{bmatrix} \hat{v}_{s1} \\ 1 \\ 0 \end{bmatrix} \tag{4-24}$$

and

$$\hat{v}_{s1} = -\left(A_a + \frac{1}{\tau_s} I \right)^{-1} B_3 \tag{4-25}$$

Similarly

$$\hat{v}_{s2} = - \left(A_a + \frac{1}{\tau_s} I \right)^{-1} B_4 \qquad (4\text{-}26)$$

Since the right eigenvectors must be perpendicular to M_3:

$$M_3 \; v_{s1} = 0 \qquad (4\text{-}27)$$

and

$$M_3 \; v_{s2} = 0 \qquad (4\text{-}28)$$

Therefore

$$M' = - M_2 \; \hat{v}_{s1} = M_2 \left(A_a + \frac{1}{\tau_s} I \right)^{-1} B_3 \qquad (4\text{-}30)$$

and

$$M'' = - M_2 \; \hat{v}_{s2} = M_2 \left(A + \frac{1}{\tau_a} I \right)^{-1} B_4$$

The matrix M_3 becomes

$$M_3 = \left[M_2 \;\middle|\; M_2 \left(A_a + \frac{1}{\tau_s} I \right)^{-1} [B_3 \; B_4] \right] \qquad (4\text{-}31)$$

For a value of $-1/\tau_s = 1.5$, the state penalty matrix becomes

$$Q_3 = \left[\begin{array}{cccc|cccc|cc}
0.0001 & 0.0000 & 0.0000 & 0.0000 & 0.0000 & 0.0000 & 0.0000 & 0.0000 & 0.0000 & 0.0000 \\
0.0000 & 0.0025 & 0.0000 & 0.0000 & 0.0000 & 0.0000 & 0.0000 & 0.0000 & 0.0023 & 0.0023 \\
0.0000 & 0.0000 & 2.0408 & 0.0000 & 0.0000 & 0.0000 & 0.0000 & 0.0000 & 0.0171 & 0.0171 \\
0.0000 & 0.0000 & 0.0000 & 8.1633 & 0.0000 & 0.0000 & 0.0000 & 0.0000 & 0.0456 & 0.0456 \\
\hline
0.0000 & 0.0000 & 0.0000 & 0.0000 & 0.1434 & -0.0015 & -0.0788 & -0.9053 & 0.0025 & -0.0025 \\
0.0000 & 0.0000 & 0.0000 & 0.0000 & -0.0015 & 2.0408 & 0.0009 & 0.0098 & -0.0033 & 0.0033 \\
0.0000 & 0.0000 & 0.0000 & 0.0000 & -0.0788 & 0.0009 & 2.0849 & 0.5061 & -0.0020 & -0.0020 \\
0.0000 & 0.0000 & 0.0000 & 0.0000 & -0.9053 & 0.0098 & 0.5061 & 13.9780 & -0.0243 & -0.0243 \\
\hline
0.0000 & 0.0023 & 0.0171 & 0.0456 & 0.0025 & -0.0033 & -0.0020 & -0.0243 & 0.0025 & 0.0024 \\
0.0000 & 0.0023 & 0.0171 & 0.0456 & -0.0025 & 0.0033 & 0.0020 & 0.0243 & 0.0024 & 0.0025
\end{array}\right] \qquad (4\text{-}32)$$

The singular values of the return difference and the loop transfer function are shown in Figs. 4-5 and 4-6 respectively. As expected the lateral loops are not affected by placing limitations on the stabilator. In the previous design, the stabilators and elevators were the major contributors to the longitudinal loop. In this design, there are two longitudinal loops - one which is predominately affected by the elevators and one which is predominately affected by the stabilators.

The singular values of the feedback system transfer function with the stabilator loops open (and all other loops closed) are shown in Fig. 4-7. The solid plot represents the collective action of the stabilator. The bandwidth of this loop is clearly within the 1.5 rad/sec bandwidth that was desired. The dotted plot represents the differential action of the stabilators, and is negligible.

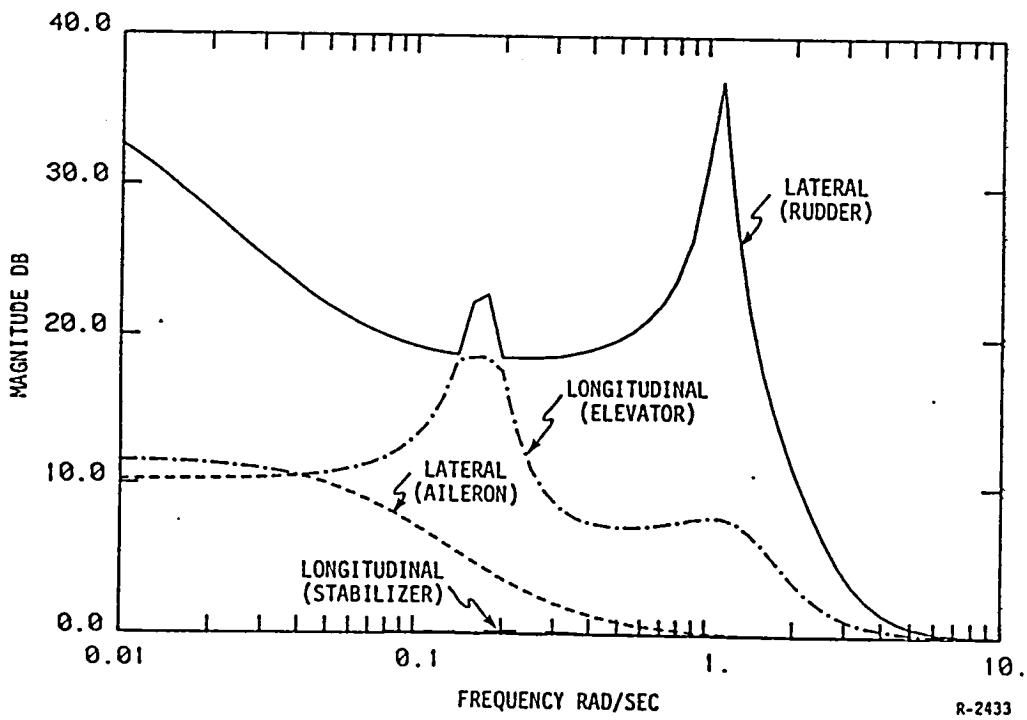

Figure 4-5. Singular Values of Return Difference for Design 3

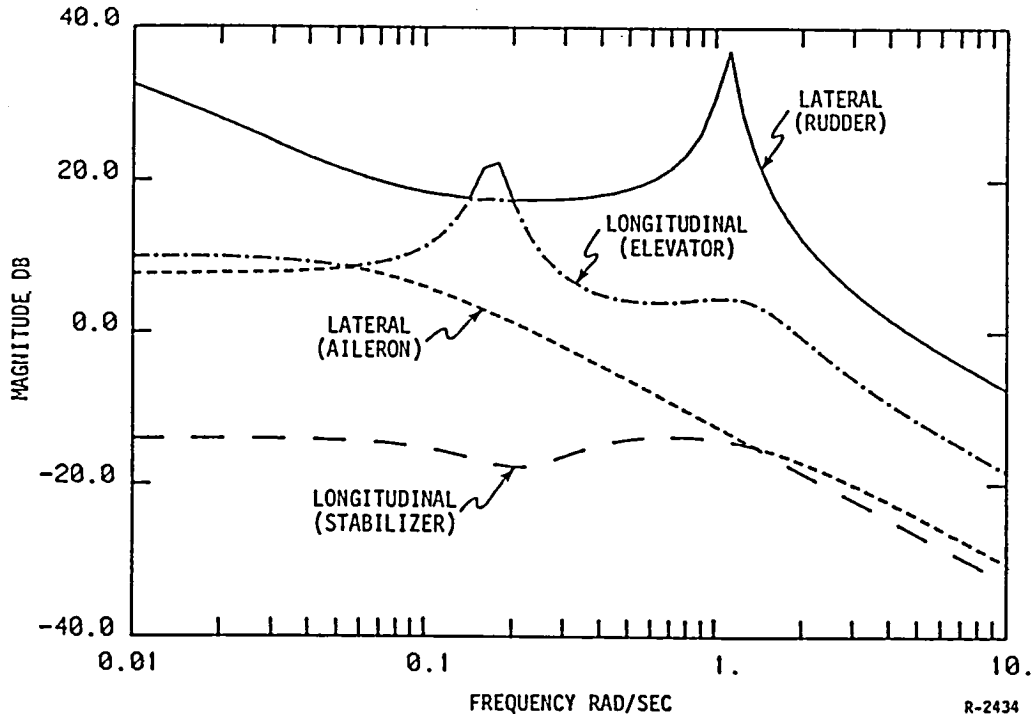

Figure 4-6. Singular Values of Loop Transfer for Design 3

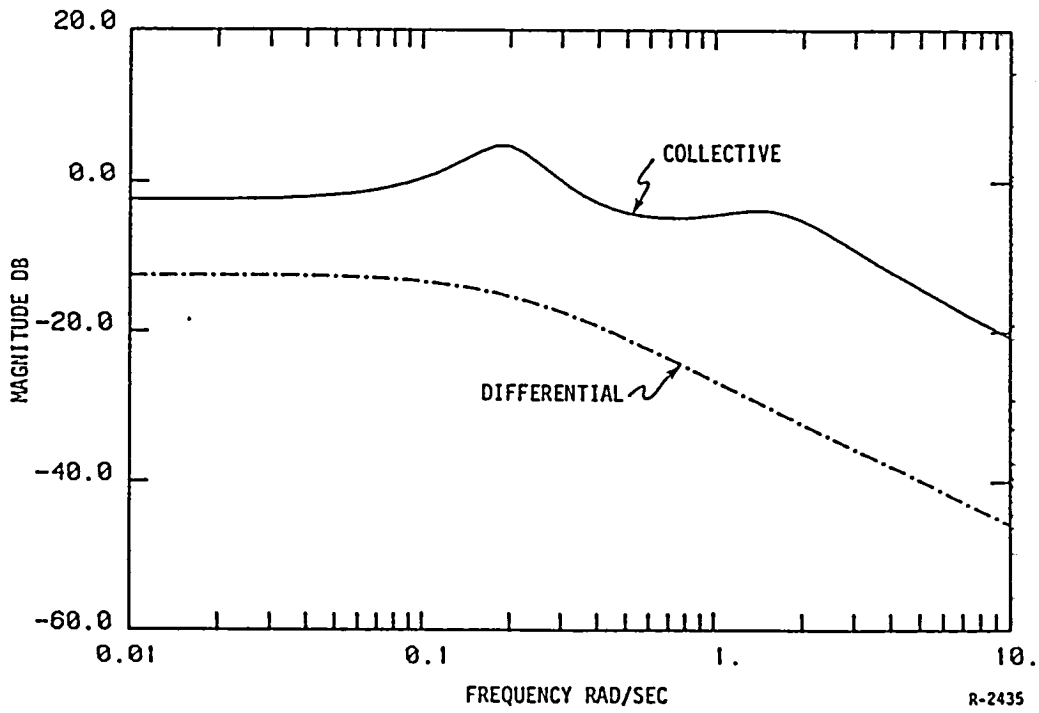

Figure 4-7. Singular Values of the Stabilizer Loop Transfer Function

The closed loop eigenvalues for this third design moved only slightly from their locations in the second design:

Short Period:	$-1.3 \pm 1.4j$
Phugoid:	$-.12 \pm .18j$
Dutch Roll:	$-2.0 \pm 2.3j$
Roll Subsidence:	-1.78
Spiral:	$-.25$
Stabilizer:	$-1.5, -1.5$

4.2.4 Integral Control

As a final step, two integrators were added to the augmented state equation to improve low frequency response to pitch and roll commands. The integral states are defined as:

$$\dot{x}_I = \begin{bmatrix} \theta \\ \phi \end{bmatrix} \triangleq C\, x_s \tag{4-33}$$

where (4-33) defines the output matrix C.

The new augmented 12 state system then becomes:

$$x \triangleq \begin{bmatrix} x_I \\ x_s \end{bmatrix} \tag{4-34}$$

$$\dot{x} = \underbrace{\begin{bmatrix} 0 & C \\ 0 & A_s \end{bmatrix}}_{A} x + \underbrace{\begin{bmatrix} 0 \\ B_s \end{bmatrix}}_{B} u_s \tag{4-35}$$

where A_s and B_s are given by (4-18)-(4-19).

The square root of the state penalty matrix will be of the form:

$$M_4 = [\, M_I \; M_2 \; M_s \,] \tag{4-36}$$

where M_I is the integrator penalty matrix, M_2 is the penalty matrix from design 2, and M_s is the stabilator penalty matrix that ensures the stabilator poles are not moved (see subsection 4.2.3). The integrator state penalty matrix will be chosen to achieve significant effects from the integrator at frequencies less than 1 rad/sec.

The LQ approximation to the loop transfer functions (4-12) with the matrices A, B, M_4, and N_4 can be used to examine the low frequency behavior of the loop transfer function. For ω small, (4-12) becomes:

$$L_c(j\omega) \approx -\frac{1}{j\omega} M_I \; [\, C \; A_s^{-1} \; B_s \,] \, N \tag{4-37}$$

Since we want the low frequency behavior to look like

$$\sigma\{\, L_c(j\omega) \,\} \approx -\frac{1}{j\omega}$$

(i.e., significant at frequencies less than 1 rad/sec), we choose M_I to set the singular values of the matrix on the right side of (4-37) to unity. If the singular value decomposition of $[\, M_2 \; A^{-1} \; B \,]$ is:

$$C \; A_s^{-1} \; B_s = U \; \Sigma \; V^H \tag{4-38}$$

we can choose M_I to be:

$$M_I = \hat{U} \; \Sigma^{-1} \; U^H \tag{4-39}$$

where $\hat{U}$ is any orthogonal matrix.

Once M_I is chosen, M_s can be specified using the procedure from subsection (4.2.3) with $[M_I \; M_1]$ replacing M_2. The quadratic state penalty matrix is then defined as:

$$Q_4 = M_4^T M_4 \tag{4-40}$$

and is given by:

$$Q_4 = \left[\begin{array}{cccccc|cccc|cc}
7.1798 & 0.0000 & 0.0000 & 0.0000 & 0.0000 & -7.6557 & 0.0000 & 0.0000 & 0.0000 & 0.0000 & -0.0160 & -0.0160 \\
0.0000 & 0.0016 & 0.0000 & 0.0000 & 0.0000 & 0.0000 & 0.0000 & 0.0010 & 0.0578 & 0.0020 & 0.0000 & 0.0000 \\
\hline
0.0000 & 0.0000 & 0.0001 & 0.0000 & 0.0000 & 0.0000 & 0.0000 & 0.0000 & 0.0000 & 0.0000 & 0.0000 & 0.0000 \\
0.0000 & 0.0000 & 0.0000 & 0.0025 & 0.0000 & 0.0000 & 0.0000 & 0.0000 & 0.0000 & 0.0000 & 0.0023 & 0.0023 \\
0.0000 & 0.0000 & 0.0000 & 0.0000 & 2.0408 & 0.0000 & 0.0000 & 0.0000 & 0.0000 & 0.0000 & 0.0171 & 0.0171 \\
7.6557 & 0.0000 & 0.0000 & 0.0000 & 0.0000 & 8.1633 & 0.0000 & 0.0000 & 0.0000 & 0.0000 & 0.0171 & 0.0171 \\
\hline
0.0000 & 0.0000 & 0.0000 & 0.0000 & 0.0000 & 0.0000 & 0.1434 & -0.0015 & -0.0788 & -0.9053 & 0.0025 & -0.0025 \\
0.0000 & 0.0010 & 0.0000 & 0.0000 & 0.0000 & 0.0000 & -0.0015 & 2.0408 & 0.0009 & 0.0098 & -0.0033 & 0.0033 \\
0.0000 & -0.0578 & 0.0000 & 0.0000 & 0.0000 & 0.0000 & -0.0788 & 0.0009 & 2.0849 & 0.5061 & -0.0020 & 0.0020 \\
0.0000 & 0.0020 & 0.0000 & 0.0000 & 0.0000 & 0.0000 & -0.9053 & 0.0098 & 0.5061 & 13.9780 & -0.0243 & 0.0243 \\
\hline
-0.0160 & 0.0000 & 0.0000 & 0.0023 & 0.0171 & 0.0171 & 0.0025 & -0.0033 & -0.0020 & -0.0243 & 0.0017 & 0.0022 \\
-0.0160 & 0.0000 & 0.0000 & 0.0023 & 0.0171 & 0.0171 & -0.0025 & 0.0033 & 0.0020 & 0.0243 & 0.0022 & 0.0023
\end{array}\right] \tag{4-41}$$

The singular values of the resulting design are shown in Figs. 4-8 and 4-9. The loop shapes are largely unaffected by the incorporation of the integral feedback with the exception of the desired low frequency gain increase and a slightly increased bandwidth. The pitch and roll response due to pitch and roll reference commands (subtracted from the state variables in the input equation) is shown in Fig. 4-10. The closed loop eigenvalues of the aircraft are:

Short Period:	$-1.2 \pm 1.4j$
Phugoid:	$-.31 \pm .30j$
Dutch Roll:	$-2.0 \pm 2.3j$
Roll Subsidence:	-1.78
Spiral:	$-.25$
Stabilators:	$-1.5, -1.5$
Roll Integrator:	$-.01$
Pitch Integrator:	$-.08$

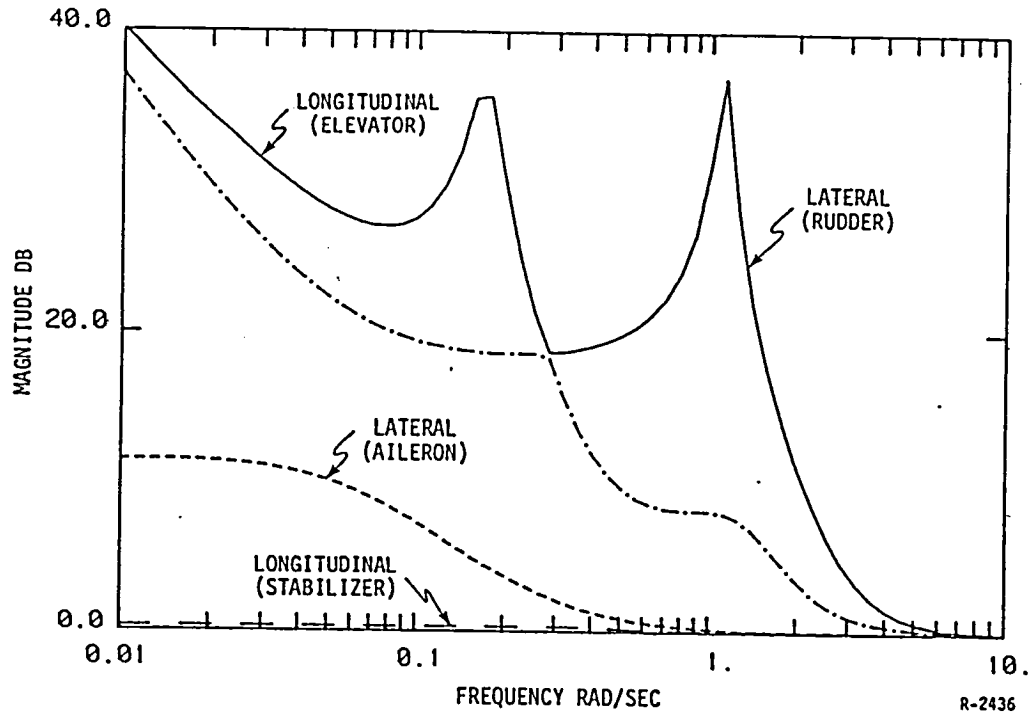

Figure 4-8. Singular Values of Return Difference for Design 4

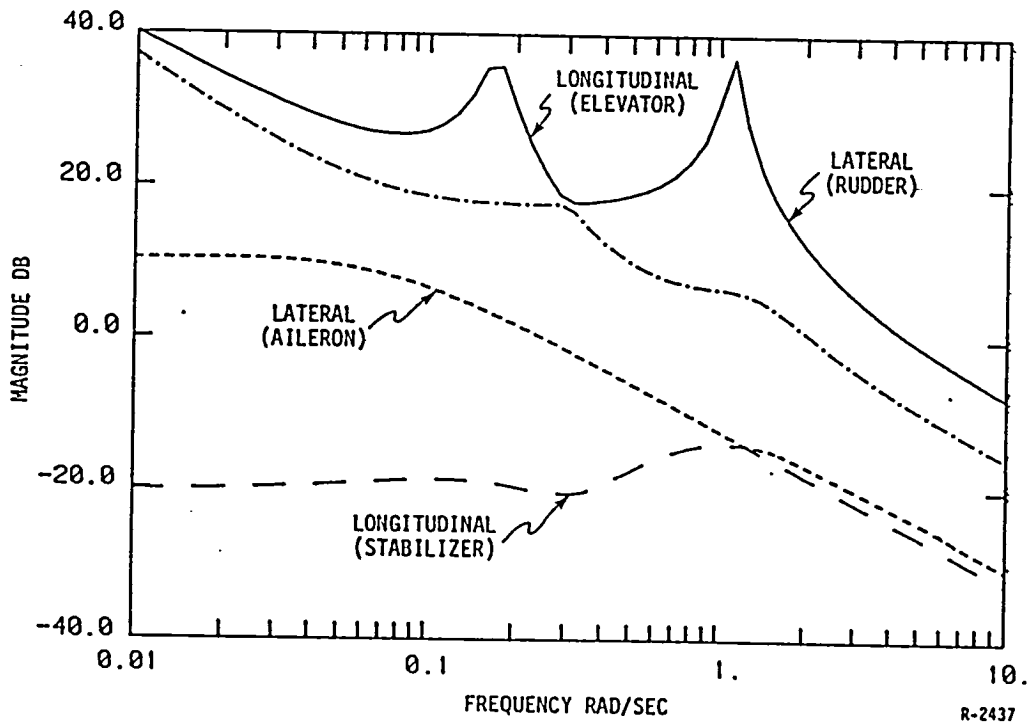

Figure 4-9. Singular Values of Loop Transfer Function for Design 4

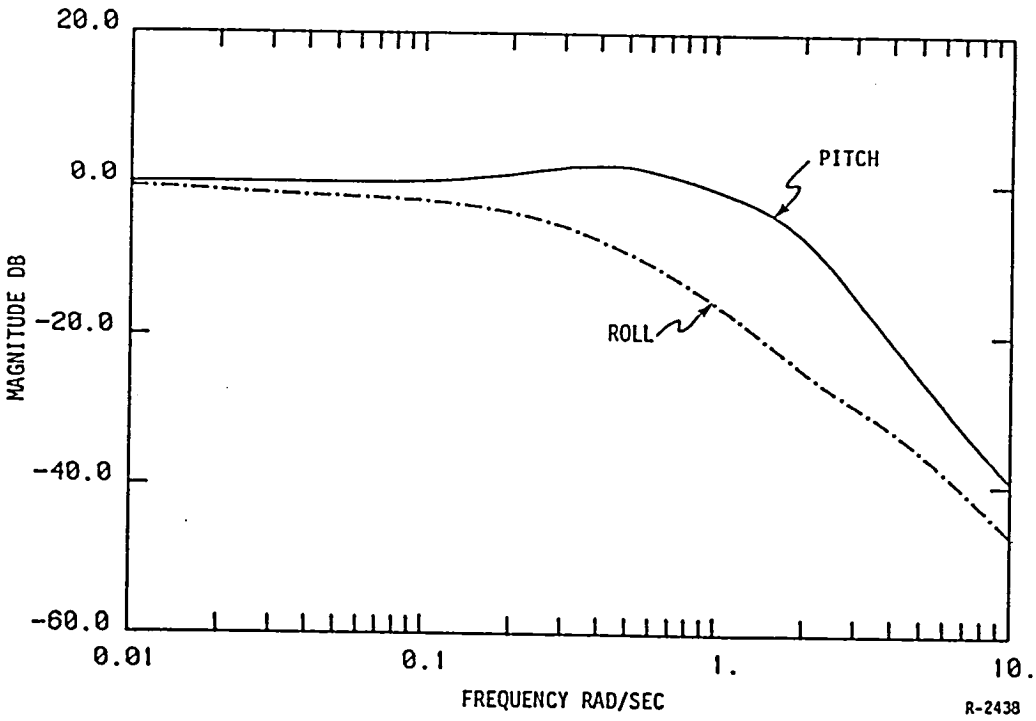

Figure 4-10. Pitch and Roll Closed Loop Transfer Functions

4.3 RESTRUCTURING FOLLOWING A RUDDER FAILURE

The linearized Boeing 737 model and the control system designed in subsection 4.2 were used to demonstrate the automatic redesign procedure. The failure that was examined was a complete failure of the rudder. The resulting closed loop Dutch roll mode after failure but before restructuring was:

$$-.08 \pm 1.1$$

The system was redesigned using the procedure described in Section 3. The Dutch roll mode of the resulting closed loop system was:

$$-.38 \pm 1.15$$

While this mode is somewhat underdamped, it is much better than the open loop mode. The singular values of the loop transfer function of the restructured system are shown in Figure 4-11. Note that the lateral singular value that

corresponded to the rudder loop in the unfailed aircraft is significantly lower than the nominal design (see Fig. 4-9).

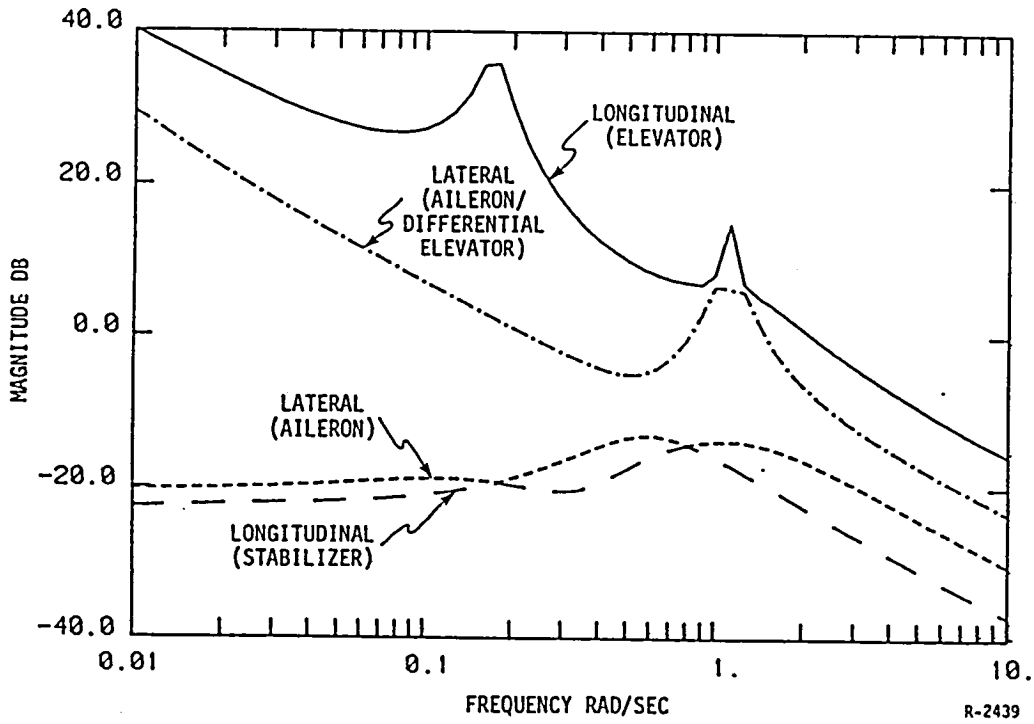

Figure 4-11. Singular Values of the Restructured System Following the Loss of the Rudder

The mechanism by which this restructuring was accomplished can be examined by studying the relative sizes of the individual components of the singular vectors. The relative sizes of these components represent the relative contribution of each surface to the singular value loop. In the unfailed aircraft, the rudder constituted nearly all the control energy in the dominant lateral loop:

Rudder - 98%

In the restructured system, the role of the rudder is assumed primarily by the ailerons with a small contribution from the elevators:

Ailerons - 84%

Elevators - 14%

A comparison of the roll responses of linearized models of the unfailed aircraft and restructured aircraft is shown in Fig. 4-12. As would be expected from a comparison of the closed loop eigenvalues, the Dutch roll mode introduces a more oscillatory response in the roll angle of the restructured aircraft. Figures 4-13 and 4-14 provide a comparison of the rudder and aileron deflections of the two configurations. These figures illustrate the replacement of the role of the rudder in the damping of the Dutch roll mode by a similar, but less effective, role for the aileron.

The unfailed and restructured aircraft were also simulated using a white noise wind model. The spectral densities of the noise processes were taken to be 2 ft/sec^2 in the horizontal and lateral axes and 1 ft/sec^2 in the vertical axis. An example of the resulting roll responses of the unfailed aircraft and the reconfigured aircraft are shown in Fig. 4-15. The response of the reconfigured aircraft is only slightly degraded from the response of the unfailed aircraft. Figures 4-16 and 4-17 again illustrate the use of ailerons in the restructured design to replace the function of the failed rudder.

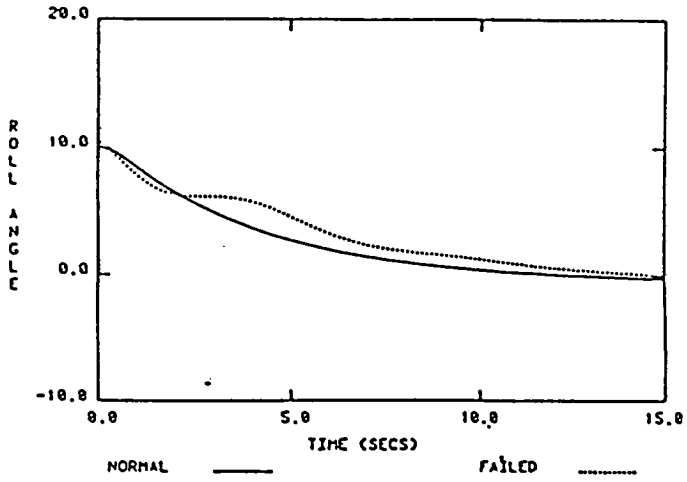

Figure 4-12. Roll Responses of the Unfailed and Restructured Aircraft to a 10° Roll Offset

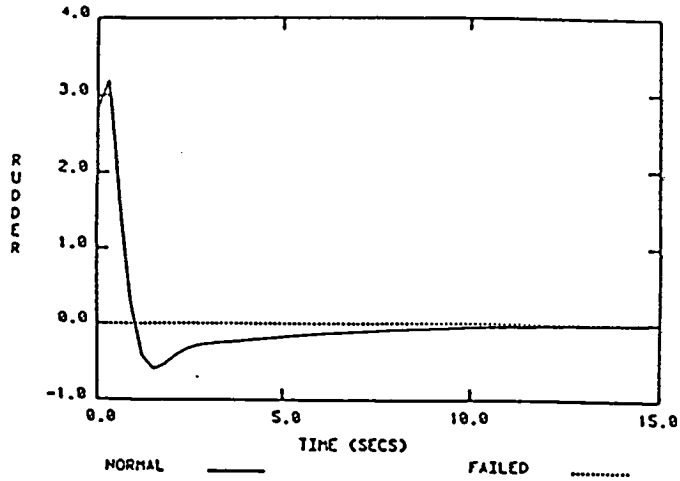

Figure 4-13. Rudder Responses of the Unfailed and Restructured Aircraft to a 10° Roll Offset

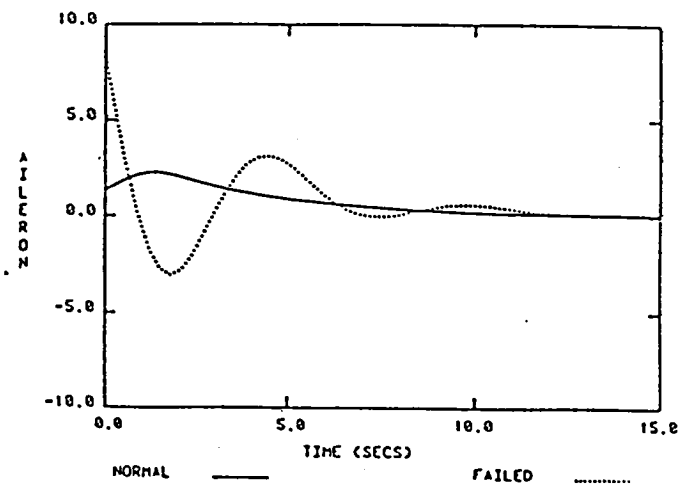

Figure 4-14. Differential Aileron Responses of the Unfailed and Restructured Aircraft to a 10° Roll Offset

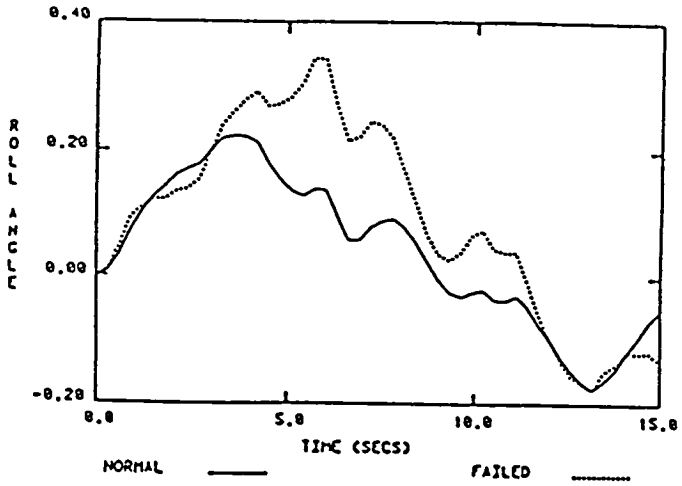

Figure 4-15. Roll Responses of the Unfailed and Restructured Aircraft to a White Noise Wind Model

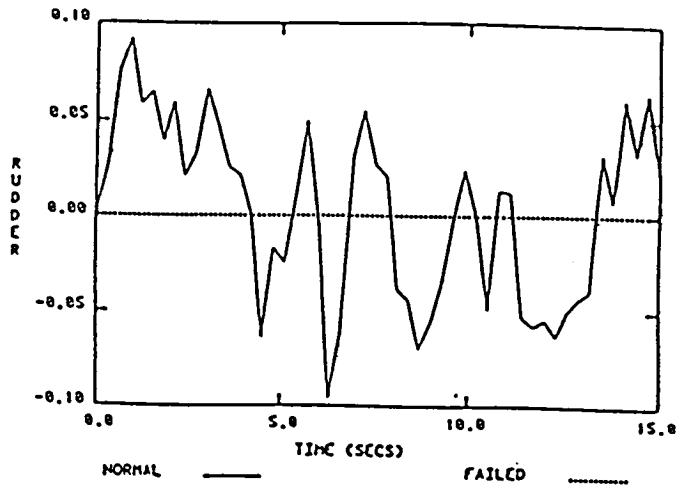

Figure 4-16. Rudder Responses of the Unfailed and Restructured Aircraft to a White Noise Wind Model

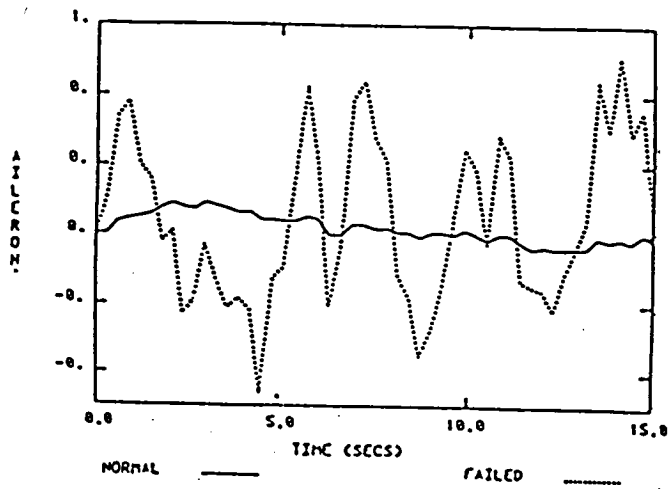

Figure 4-17. Aileron Responses of the Unfailed and Restructured Aircraft to a White Noise Wind Model

SECTION 5

APPLICATION TO AN ADVANCED FIGHTER AIRCRAFT

The automatic redesign procedure was demonstrated on an ATF class fighter aircraft to illustrate its ability to successfully handle higher bandwidth, open loop unstable systems. The model used for this demonstration is the Northrop Design Methods for Integrated Control Systems (DMICS) model, which is a modification of the FA-18/A. The control configuration used was the standard FA-18/A configuration augmented with horizontal canards. The linearized dynamics were obtained at MACH .8 and 10,000 feet with a trim angle of attack of 1.3°. The aircraft at this flight condition is open loop unstable, with the open loop poles being:

Short Period	2.8, -5.9
Phugoid:	$-.019 \pm .026j$
Dutch Roll:	$-.44 \pm 2.6j$
Spiral:	-.01
Roll Subsidence:	-3.7552

A simplified regulator design with a limited set of performance specifications was developed using LQ design techniques to illustrate the redesign procedure. The dominant singular values of the loop transfer function of the unfailed aircraft are shown in Fig. 5-1. The closed loop eigenvalues are:

Short Period: $-5.0 \pm 2.0j$ Dutch Roll: $-2.9 \pm 3.9j$.

The relative contributions of each of the surfaces to the longtitudinal singular value are: Right Stabilator-39%; Left Stabilator-39%; Right Canard-10%; Left Canard-10%.

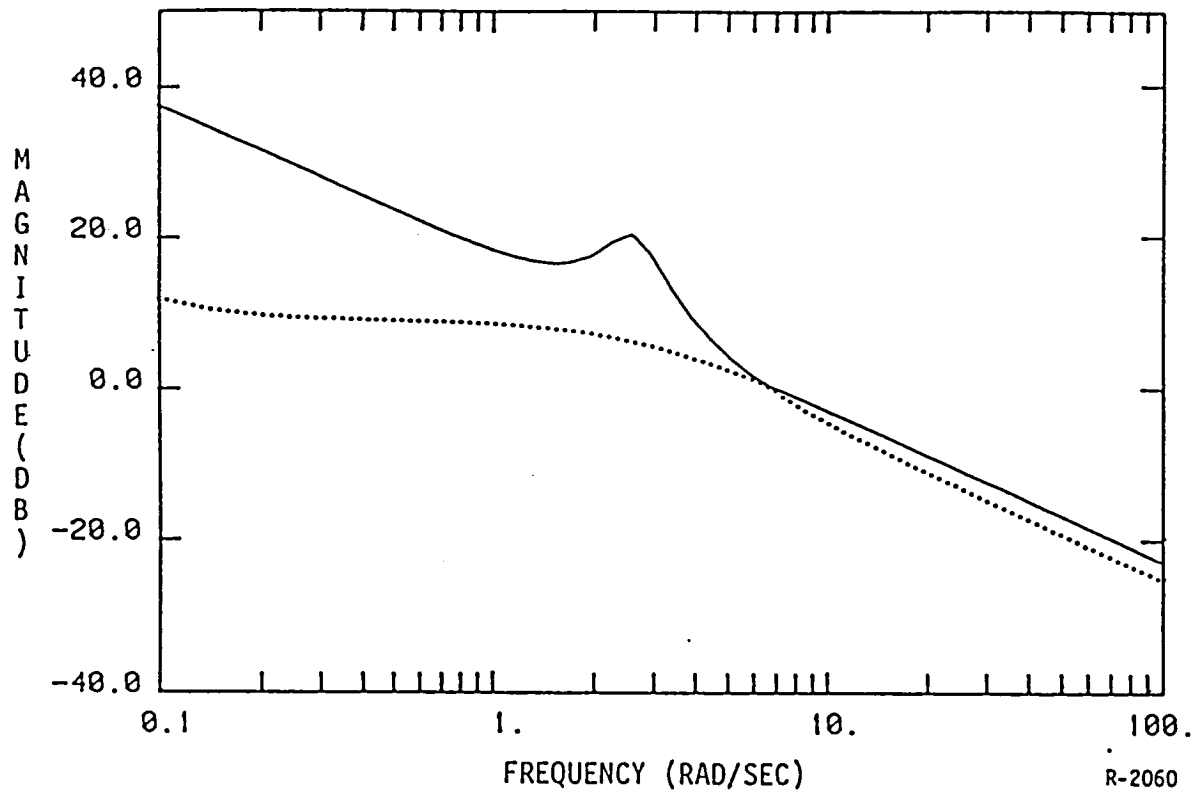

Figure 5-1. Dominant Lateral (——) and Longitudinal (•••) Loop Singular Values of the Unfailed Aircraft

Following a failure of the right stabilator, the FCS was reconfigured using the automatic redesign algorithm. The dominant singular values of the loop transfer function of the reconfigured aircraft are shown in Fig. 5-2. Note that the reconfigured singular values are virtually indistinguishable from those of the unfailed aircraft. The closed loop eigenvalues also remain virtually unchanged. The relative contributions of each surface are: Right Canard-45%; Left Stabilator-43%; Left Candard-3%. Note that the reconfiguration has redistributed the responsibility for longitudinal stabilization and pitch control to the remaining effectors in the longitudinal system.

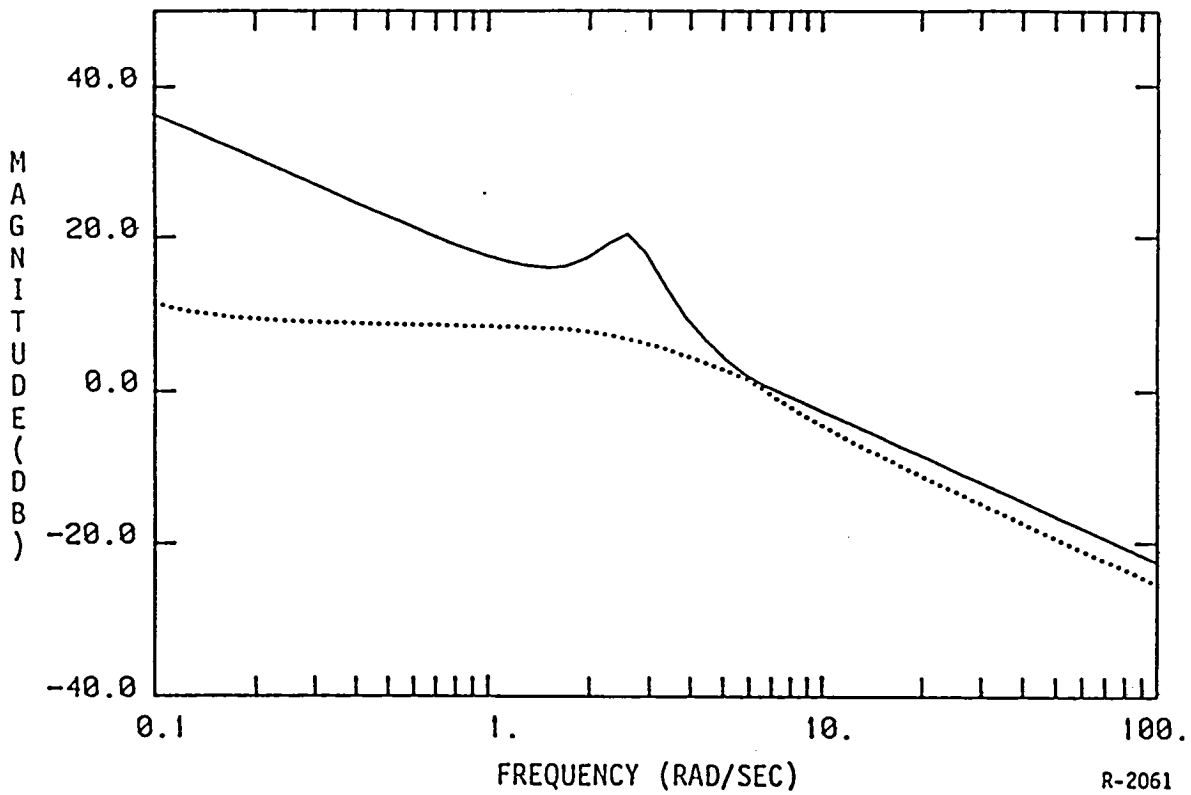

Figure 5-2. Dominant Lateral (——) and Longitudinal (•••) Loop Singular Values of the Reconfigured Aircraft Following a Right Stabilator Failure

The left stabilator of the aircraft was then failed (resulting in both stabilators missing). The dominant singular values of the loop transfer function of the reconfigured aircraft are shown in Fig. 5-3. The longitudinal singular value is noticeably lower than the corresponding value of the unfailed aircraft in Fig. 5-1, but is still acceptable. The closed loop eigenvalues are:

Short Period: $-5.3 \pm -3.8j$ Dutch Roll: $-2.9 \pm 3.9j$.

The relative contributions of the surfaces with both stabilators failed is: Right Canard-45%; Left Canard-45%; Leading Edge Flaps-4%; Ailerons-4%.

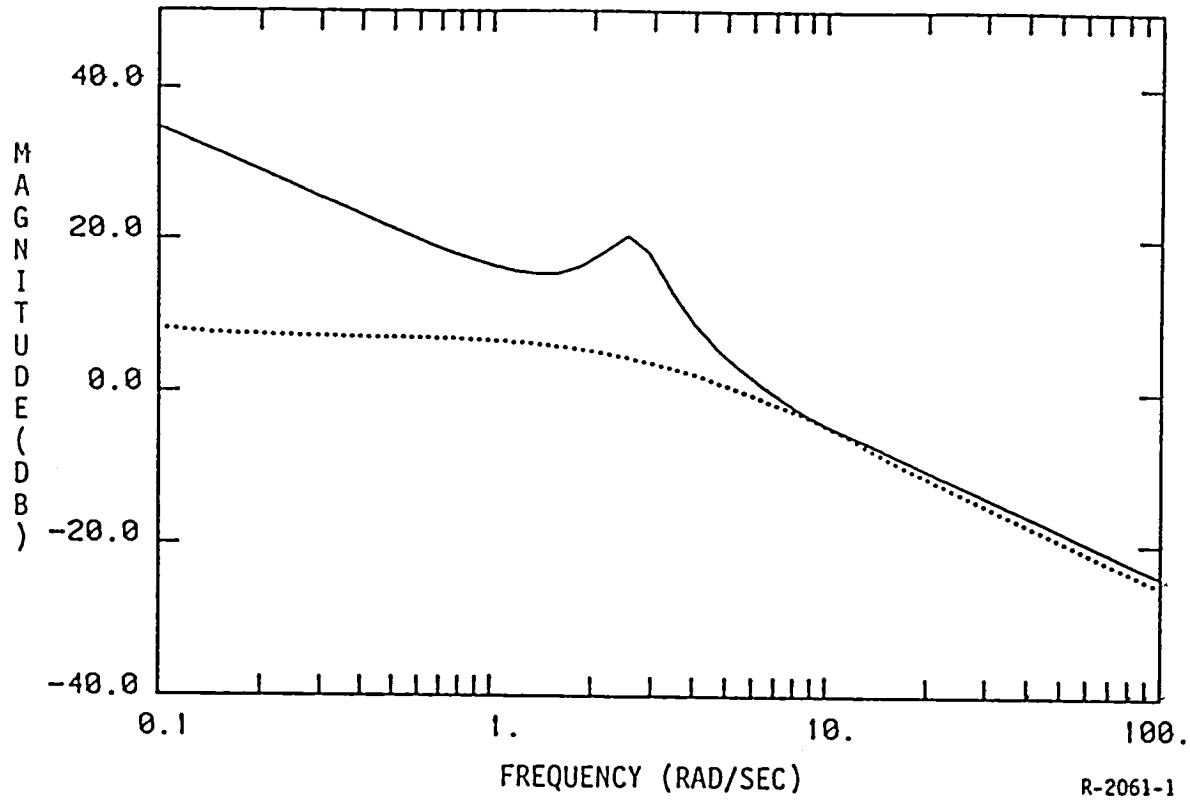

Figure 5-3. Dominant Lateral (——) and Longitudinal (•••) Loop Singular Values of the Reconfigured Aircraft Following Failures of Both Stabilators

In each of these cases the lateral singular value was virtually unaffected. The principal reason for this is that this loop approximately corresponds to a yaw damping loop. The stabilators have only a relatively minor contribution (~20%) to this loop, and can be readily replaced by redistributing authority to the rudders and ailerons.

SECTION 6

SUMMARY AND FUTURE WORK

This report has presented the development and preliminary demonstration of an automatic redesign algorithm for restructurable flight control systems. The automatic redesign procedure possesses a number of highly desirable features. The procedure was developed from an optimization formulation that attempts to maximize a measure of feedback system performance while satisfying the bandwidth limitations of the control system. As a result, the procedure can be interpreted as reconstructing the nominal forces and moments of the unfailed aircraft as nearly as possible. In addition, the control effector bandwidths can be explicitly incorporated in the redesigned system. By using the nominal control system design parameters as a basis for the redesign, the procedure effectively transfers the engineering trade-offs used in the control system design for the unfailed aircraft to the restructured control system design. The performance of the restructured design degrades gracefully (while maintaining robustness margins) as the severity of the failure increases. Since the algorithm recovers the design parameters of the unfailed systems when supplied with the unfailed system model, the original FCS is also recovered. Finally, the ability to incorporate failure detection estimates in the FCS restructuring helps to reduce the requirements placed on the FDI algorithm and can enhance the reliability of the restructuring system.

In addition to restructuring of the dynamic compensation to provide stability and dynamic disturbance rejection, a restructurable control system must be able to automatically trim the aircraft. The automatic trim problem has two important facets: a linearized trim problem for rejecting disturbances while maintaining a specified flight condition; and the problem of choosing the flight condition (operating point) to provide the greatest safety and flying qualities. While the first problem was discussed briefly in Section 2, only a formal solution was presented. This solution certaintly requires further study. The nonlinear problem of choosing a flight condition has not yet been addressed. Finally, each of the individual modules will have to be combined with a FDI system to produce a truly restructurable control system.

REFERENCES

1. "National Transportation Safety Board Accident Report of the American Airlines DC10 Crash at Chicago - O'Hare International Airport, May 25, 1979," NTSB-AAR-79-17, December 21, 1979.

2. McMahan, J. "Flight 1080," Air Line Pilot, July 1978.

3. Montoya, R.J, W.E. Howell, W.T. Bundick, A.J. Ostroff, R.M. Hueschen, and C.M. Belcastro, Restructurable Controls, NASA Conference Publication 2227, NASA Langley Research Center, Hampton, Virginia, September 21-22, 1982.

4. Willsky, A.S., "A Survey of Design Methods for Failure Detection in Dynamic Systems," Automatica, Volume 12, 1976, pp. 601-611.

5. Sain, M.K., ed., Special Issue on Linear Multivariable Systems, IEEE Trans. A.C., Volume AC-26, No. 1, February 1981.

6. Smith, H.W. and E.J. Davison, "Design of Industrial Regulators," Proc. IEEE, Volume 119, No. 8, August 1972.

7. Horowitz, I.M., Synthesis of Feedback Systems, Academic Press, New York, 1963.

8. Doyle, J.C. and G. Stein, "Multivariable Feedback Design: Concepts for a Classical/Modern Synthesis," IEEE Trans. A.C., Volume AC-26, No. 1, February 1981.

9. Cruz, J.B., J.S. Freudenberg, and D.P. Looze, "A Relationship Between Sensitivity and Stability of Multivariable Feedback Systems," IEEE Trans. A.C., Volume AC-26, No. 1, February 1981.

10. Safonov, M.G., A.J. Laub, and G.L. Hartman, "Feedback Properties of Multivariable Systems: The Role and Use of the Return Difference Matrix," IEEE Trans. A.C., Volume AC-26, No. 1, February 1981.

11. Kalman, R.E., "When is a Linear Control System Optimal?" Journal of Basic Eng., Trans. of ASME, Series D, Volume 86, March 1964.

12. Smith, B.T., et al., Matrix Eigensystem Routines - EISPACK Guide, 2nd Edition, Lecture Notes in Computer Science, Volume 6, Springer-Verlag, New York, 1976.

13. Athans, M., "The Role and Use of the Stochastic Linear - Quadratic - Gaussian Problem in Control System Design," IEEE Trans. A.C., Volume AC-16, No. 6, December 1971.

14. Ostroff, A.J. and R.M. Hueschen, "Investigation of Control Law Reconfiguration to Accommodate a Control Element Failure on a Commercial Airplane," 1984 ACC, San Diego, CA, June 6-8, 1984.

1. Report No.	2. Government Accession No.	3. Recipient's Catalog No.
NASA CR - 172489		

4. Title and Subtitle	5. Report Date
Automatic Control Design Procedures for Restructurable Aircraft Control	January 1985
	6. Performing Organization Code
7. Author(s)	8. Performing Organization Report No.
D.P. Looze, S. Krolewski, J. Weiss, N. Barrett, J. Eterno	TR - 212-1
9. Performing Organization Name and Address	10. Work Unit No.
ALPHATECH, Inc. 111 Middlesex Turnpike Burlington, MA 01803	11. Contract or Grant No. NAS1 - 17411
12. Sponsoring Agency Name and Address	13. Type of Report and Period Covered
National Aeronautics and Space Administration Langley Research Center Hampton, VA 23665	Contractor Report
	14. Sponsoring Agency Code

15. Supplementary Notes

Langley Technical Monitor: Aaron Ostroff

Final Report

16. Abstract

The primary contribution of this report is the development and preliminary analysis of a simple, reliable automatic redesign procedure for restructurable control. This procedure is based on Linear Quadratic (LQ) design methodologies. It employs a robust control system design for the unfailed aircraft to minimize the effects of failed surfaces and to extend the time available for restructuring the Flight Control System. The procedure uses the LQ design parameters for the unfailed system as a basis for choosing the design parameters of the failed system. This philosophy allows the engineering trade-offs that were present in the nominal design to be inherited by the restructurable design. In particular, it allows bandwidth limitations and performance trade-offs to be incorporated in the redesigned system.

The procedure also has several other desirable features. It effectively redistributes authority among the available control effectors to maximize the system performance subject to actuator limitations and constraints. It provides a graceful perfomance degradation as the amount of control authority lessens. When given the parameters of the unfailed aircraft, the automatic redesign procedure reproduces the nominal control system design. The procedure can incorporate the uncertainty of the aircraft control and stability derivatives that may arise from the use of nonstandard control configurations or from estimates of these derivatives supplied by the FDI algorithim. Finally, the procedure is conceptually simple, easily implemented, and computationally fast.

17. Key Words (Suggested by Author(s))	18. Distribution Statement
Restructurable Flight Control Automatic Control Design	Unclassified - Unlimited

19. Security Classif. (of this report)	20. Security Classif. (of this page)	21. No. of Pages	22. Price
Unclassified	Unclassified	65	

DO NOT REMOVE SLIP FROM MATERIAL

Delete your name from this slip when returning material to the library.

NAME	MS
~~Stabrino~~	149
LIBRARY	185

NASA Langley (Rev. May 1988) RIAD N-75